Optimal Investment Strategies for Power Generation: the Value of Green Energy

Jerome Detemple & Yerkin Kitapbayev

31 August 2017

This paper examines the investment in and the valuation of power generation projects under uncertainty. The analysis incorporates the possibility of producing from alternative types of fuels, such as renewables (wind) or fossil fuels (gas), hence alternative types of plants/technologies. We show that the optimal investment decision can be characterized by two boundaries that satisfy a system of coupled integral equations of Fredholm type and propose a numerical algorithm for resolution. The value of a license to produce from the best of the two types of plants is the premium associated with the optimal investment policy, i.e., the present value of the cumulative instantaneous gains realized when either of the two technologies is optimal. The ability to select the type of plant/technology has significant effects on investment in power generation. The option to produce power from renewables, as opposed to fossil fuels, increases the value of power generation projects and postpones the optimal investment time. The optimal delay can be substantial even if the spark spread and the price of electricity are both large. The premium from renewables can be positive, even when the current value of fossil fuel power plants exceeds that of renewables power plants. Green power generation emerges as a significant source of value creation.

JEL Classification: G13, Q40, Q42, L94.
Key Words: spark spread, power plant, gas-fired, renewable energy, wind.

1. Introduction

In recent years renewables have become the fastest growing sources of energy in the world. In 2014, they accounted for 19.2% of the global final energy consumption, whereas fossil fuels and nuclear represented 78.3% and 2.5%, respectively (REN21 (2016)). Renewables have become especially important for power generation. Growth rates of power production capacity from Wind (W), Solar Photovoltaic (SPV) and Concentrated Solar Power (CSP) reached 17%, 28% and 9.7% in 2015. That year, renewables accounted for about 23.7% of global electricity production.

The increased use of renewables for power generation is tied to several developments. Overall, renewables are becoming more competitive sources of electricity production. For instance, the efficiency of solar and wind production technologies has increased and, at the same time, the prices of certain system components (e.g., solar panels) have come down. Second, emission costs and CO2 capture technologies are adding to the expenses affecting generation from tra-

ditional fuels. Finally, subsidies in the form of price premia and tax rebates have been widely implemented to provide incentives for the use of renewables. As a result of these developments, the cost per MWh of renewable power generation has decreased to levels that are closer to those of fossil fuel generation. It is especially noteworthy that renewables remain competitors of fossil fuels even in the face of sharp recent decreases in the prices of certain fuels (e.g., oil, natural gas, etc...).

In light of these developments, power plant operators are now faced with non-trivial choices between competitive technologies when they invest in new production units. On the one hand they can build plants using traditional fuels to generate power (e.g., gas-fired plants). On the other hand they can use renewables (e.g., wind plants). These decisions are complex as they involve different types of price uncertainties as well as different technologies. Moreover, choices have long-lasting implications: they lock operators in a technological space for substantial amounts of time (the typical life of a power plant is in the 20-25 years range). Ultimately, choices between technologies have critical implications for societies as they affect global warming and related phenomena.

This paper seeks to examine these issues. Our main goal is to understand the choice between different types of power production technologies. We focus on gas-fired plants as the representative power generation source for traditional fuels. This reflects the fact that natural gas has become the most efficient source of power production from fossil fuels. The representative renewables source considered is wind. Wind power was the second fastest growing segment in that space (behind SPV) and had the second highest share of global electricity production of all renewables (behind hydropower) in 2015. We thus consider an operator with a license to build a power plant and who seeks to choose between building a gas-fired plant or a wind plant.[1] As licenses are typically valid for extended periods of time, the timing of the decision to build is flexible. Moreover, each of these selections involves subsequent timing choices regarding operations. Hence, the license holder holds an American-style real option on the maximum of two asset values, which are themselves American-style contingent claims. Some of the fundamental questions that emerge in this context are the following. What is the optimal timing of the decision to build? Under what conditions is it optimal to invest in power production from renewables? Are current incentive schemes sufficient to spur investment in this sector? What is the sensitivity of investments in power generation with respect to relevant determinants, e.g., price uncertainties, interest rates, incentives and technological parameters. Answers to these questions are important not only for operators but also for consumers and policy makers.

The model developed considers two underlying sources of uncertainty, the spark spread and the price of electricity. The spark spread, i.e., the difference between the prices of electricity and gas, drives the value of gas-fired power plants. The price of electricity is the main factor underlying the value of wind farms. Our first result shows that the decision to invest can be characterized by two boundaries. When the spark spread exceed the first boundary, then immediate investment in a gas-fired plant is optimal. When the price of electricity exceeds the second boundary it is optimal to invest in a wind plant. Each of these boundaries depends on the other source of uncertainty. For instance the boundary for optimally investing in a wind plant depends on the spark spread. Hence, the two boundaries are stochastic. We show that

[1] A project involving decisions to time investment and select between competing technologies is equivalent to a license to choose the best technology.

they satisfy a system of coupled integral equations of Fredholm type. Although these equations are non-recursive in nature, we are able to design a new iterative algorithm to compute the boundaries.

A license to invest in power generation from the best production technology is an American-style dual strike compound max-option. It is a compound option because the value of a gas-fired plant embeds options to shut down or restart production when the spark spread reaches certain thresholds, hence is inherently nonlinear. It is a dual strike option because the cost of building a gas-fired plant differs from the cost of building a wind farm. Finally, it is a max-option because of the availability of competing technologies for power production. We show that the value of a perpetual license has an Early Investment Premium (EIP) representation. That is, it can be written as the present value of the cumulative local gains realized by optimally investing in the best technology. This premium splits as a premium for investing when the gas-fired plant is optimal and one for investing when the wind farm is optimal. Each of these components is parametrized by both exercise boundaries, reflecting the inherent interdependence between the two decisions. As the boundaries can be computed, the value of the license can be calculated as well.

The optimal investment decision has notable features. First, it is suboptimal to invest if the values of the two underlying plants coincide. This is true even if both values are extremely large. In these instances, it pays to delay investment even though it would be optimal to invest when a given technology is considered in isolation. The premium associated with the optimal investment delay is substantial. Numerical experiments show that it can double the value of a license over typical ranges of spark spread values. Second, it remains optimal to delay investment even if one of the projects has significantly more value than the other one. In fact, we identify a cone within which immediate investment is suboptimal. The edges of this cone diverge as the spark spread and the price of electricity increase. This means that the value of waiting can remain positive even when the difference between the underlying factors increases to infinity, i.e., when one project becomes infinitely more valuable than the other one. Thus, there are economic benefits to consider green power generation in investment decisions even if the current value of fossil fuel plants substantially exceeds that of renewables power plants.

The availability of production technologies based on renewables increases the value of power projects and operators' licenses. The mere possibility of building a wind farm as opposed to being locked into a gas plant investment can raise value by a factor of 10. The wind premium can be large and, for a fixed price of electricity, it decreases slowly as the spark spread increases. It also increases when the volatility of the electricity price increases and when the cost of investing decreases.

To our knowledge, this paper is the first one to incorporate the option to select between different types of technologies in the valuation of power projects and to examine the value added by considering production from renewables. The previous literature dealing with power generation focuses on projects using a given technology. Fleten and Nasakkala (2004) study investment timing and operating policies for gas-fired plants. Deng, Johnson and Sogomonian (1999) and Maribu, Galli and Armstrong (2007) price spark spread options. This literature considers various processes for underlying prices/spreads, including arithmetic Brownian motions. Fleten, Maribu and Wangensteen (2007) examine investments in renewables power generation. Boomsma, Meade and Fleten (2012) allow for capacity choice in addition to timing and study the impact of different types of renewables support schemes. Both assume that underlying

prices are geometric Brownian motions.

The problem considered in this paper involves two underlying processes, for the spark spread and the electricity price, as well as embedded optimal stopping time problems for the operating decisions of the gas plant and the timing and selection decisions of the power plant operator. In order to keep the analysis as simple as possible, yet analytically tractable, we are led to model the spark spread directly, assuming an arithmetic Brownian motion. For the electricity price we use a geometric Brownian motion as is standard in the literature on renewables power generation. We also consider an extension to an Ornstein-Uhlenbeck process for the spark spread to capture mean reversion. Specifications involving mean reverting processes for electricity prices are common in the literature and supported by empirical evidence (see Lucia and Schwartz (2002) and Geman and Roncoroni (2006)).

The paper is also related to broader literatures on real options and American option pricing. Seminal contributions in the real option area highlight the values of flexibility and of waiting to invest (e.g., Brennan and Schwartz (1985), McDonald and Siegel (1985, 1986); see also Dixit and Pyndick (1994) and references therein). This literature relies on option pricing methods and partial differential equations to price projects. In contrast, we exploit a characterization of the value function based on the EIP representation, which is rooted in probabilistic/martingale methods (see Kim (1989) and Carr, Jarrow and Myneni (1992) for American options). We also extend the literature on the valuation of multiasset American claims (e.g., Broadie and Detemple (1997)), by considering dual strike compound max-options and designing a new implementable algorithm that solves systems of coupled integral equations of Fredholm type for optimal exercise boundaries. The advantage of our algorithm compared to, e.g., PDE or Monte-Carlo methods, is the ability to tackle perpetual or long horizon problems. This approach can help to address other challenging multidimensional stopping problems with applications, e.g., in real options theory and American option pricing theory.

Section 2 develops the model for electricity production using traditional fuels. Section 3 examines the case of production from renewables. Section 4 solves for the value of an investment project in power generation when alternative technologies are available and studies the optimal investment strategy. An extension of the basic model is in Section 5. Conclusions follow. Proofs are in the Appendix.

2. Production from traditional fuels: gas-fired plant

Gas-fired plants are currently the most efficient at producing electricity from traditional fuels. Our model for traditional fuels uses that technology as benchmark. Production and prices are described in Section 2.1. The solution is provided in Section 2.2. Economic insights are reported in Section 2.3.

2.1. Production and spark spread modeling

The operation of a gas-fire plant.generates a cash flow equal to the spread between the electricity price and the cost of fuels, in this instance gas. The spread, which is called the spark spread, equals $X = Y - \kappa G$, where Y, G are the respective prices of electricity and gas, and κ is the heat rate, i.e., the amount of gas necessary to generate $1MWh$ of electricity. To simplify the analysis, we model the spark spread directly, assuming that it follows an arithmetic Brownian

motion (ABM) with drift under risk-neutral measure,

$$dX_t = \mu_X dt + \sigma_X dB_t, \quad X_0 = x,$$

where B is a standard Brownian motion, and the parameters μ_X and $\sigma_X > 0$ represent the drift and volatility, respectively. An extension to a more complex model of the spark spread, with mean reversion, can be found in Section 5.

The production model assumes that the gas-fired plant can operate indefinitely (infinite horizon) and that it can be in two states: idle (0) and operating (1). There are running cost rates k_0 and k_1 associated with each state, and there are also fixed switching costs c_0 and c_1, to pass from state 0 to 1 and conversely. The value of the plant in each state can therefore be described as follows,

$$V_0(x) = \sup_{\tau \geq 0} \mathsf{E}_x \left[- \int_0^\tau e^{-rs} k_0 ds + e^{-r\tau}(V_1(X_\tau) - c_0) \right] \tag{2.1}$$

$$V_1(x) = \sup_{\zeta \geq 0} \mathsf{E}_x \left[\int_0^\zeta e^{-rs}(X_s - k_1) ds + e^{-r\zeta}(V_0(X_\zeta) - c_1) \right] \tag{2.2}$$

for $x \in I\!R$. The value of the plant in the idle state, $V_0(x)$ consists in two parts. The first one is the present value of the maintenance cost incurred until operation resumes. The second one is the value created by resuming operations at the future time τ, i.e., the value of the option to resume. The plant maximizes value by choosing the best time τ to resume operations. Likewise, the value $V_1(x)$ of the plant in the operating mode has two components: the value of the net spark spread $X - k_1$ collected while running the plant and the value of idling at the future time ζ, i.e., the value of the option to idle. Value is maximized by choosing the best time ζ to idle. As the timing of the options to operate and idle are endogenous, the two options are American-style. The two values depend on each other. The pair $(V_0(x), V_1(x))$ solves the coupled optimal stopping time problem described above.

2.2. Solving the gas-fired plant problem

The operator of the plant has the possibility of switching back and forth between the two states of operation described above. The optimal switching decisions are determined by two thresholds, $b_0 > b_1$. When the plant is idle, it becomes optimal to turn the system on when X_t hits b_0 from below. When it operates, it becomes optimal to cease production when X_t reaches b_1 from above.

Standard arguments show that the value of idling satisfies the following ODE,

$$\frac{\sigma_X^2}{2} V_0''(x) + \mu_X V_0'(x) - r V_0(x) - k_0 = 0$$

for $x < b_0$. The general solution to this ODE is given by,

$$V_0(x) = A_0 e^{\alpha x} + B_0 e^{\widetilde{\alpha} x} - \frac{k_0}{r}$$

where A_0, B_0 are constants, and $\widetilde{\alpha} < 0 < \alpha$ are the roots of the quadratic equation,

$$\frac{\sigma_X^2 \alpha^2}{2} V_0''(x) + \mu_X \alpha - r = 0.$$

As V_0 is bounded, we have that $B_0 = 0$ and thus,

$$V_0(x) = A_0 e^{\alpha x} - \frac{k_0}{r}$$

for $x < b_0$. It is also clear that $V_0(x) = V_1(x) - c_0$ for $x \geq b_0$ and both continuity and smooth pasting conditions hold at b_0.

Likewise, the value of operating satisfies,

$$\frac{\sigma_X^2}{2} V_1''(x) + \mu_X V_1'(x) - r V_1(x) + x - k_1 = 0$$

for $x > b_1$. The solution to this ODE is given by,

$$V_1(x) = B_1 e^{\widetilde{\alpha} x} + \frac{x + \mu_x/r - k_1}{r}$$

as V_1 is bounded and where B_1 is some constant. We also have that $V_1(x) = V_0(x) - c_1$ for $x \leq b_1$. Again, continuity and smooth fit conditions are satisfied at b_1.

Given the candidate value functions above and using the continuity and smooth pasting conditions at b_0 and b_1, leads to the system of four algebraic equations with four unknown variables (b_0, b_1, A_0, B_1),

$$A_0 e^{\alpha b_0} - \frac{k_0}{r} = B_1 e^{\widetilde{\alpha} b_0} + \frac{b_0 + \mu_x/r - k_1}{r} - c_0 \tag{2.3}$$

$$\alpha A_0 e^{\alpha b_0} = \widetilde{\alpha} B_1 e^{\widetilde{\alpha} b_0} + \frac{1}{r} \tag{2.4}$$

$$B_1 e^{\widetilde{\alpha} b_1} + \frac{b_1 + \mu_x/r - k_1}{r} = A_0 e^{\alpha b_1} - \frac{k_0}{r} - c_1 \tag{2.5}$$

$$\widetilde{\alpha} B_1 e^{\widetilde{\alpha} b_1} + \frac{1}{r} = \alpha A_0 e^{\alpha b_1}. \tag{2.6}$$

Clearly, this system has a unique solution and can be solved numerically. The standard verification arguments shows that the solution to this system provides the value functions and optimal operation rules in (2.1)-(2.2).

To summarize, we have shown the following representations for the value functions,

$$V_0(x) = \begin{cases} A_0 e^{\alpha x} - \frac{k_0}{r}, & x < b_0 \\ B_1 e^{\widetilde{\alpha} x} + \frac{x + \mu_x/r - k_1}{r} - c_0, & x \geq b_0 \end{cases}$$

$$V_1(x) = \begin{cases} B_1 e^{\widetilde{\alpha} x} + \frac{x + \mu_x/r - k_1}{r}, & x > b_1 \\ A_0 e^{\alpha x} - \frac{k_0}{r} - c_1, & x \leq b_1 \end{cases}$$

2.3. The value of a gas-fired plant

The value of the gas-fired plant is an increasing convex function of the spark spread. Figure 1 shows the value function V_1 in the operating state versus the value V_{cont} of continuous operation, i.e.,

$$V_{cont}(x) = \mathsf{E}_x \left[\int_0^\infty e^{-rs} (X_s - k_1) ds \right] = \frac{x + \mu_x/r - k_1}{r} \tag{2.7}$$

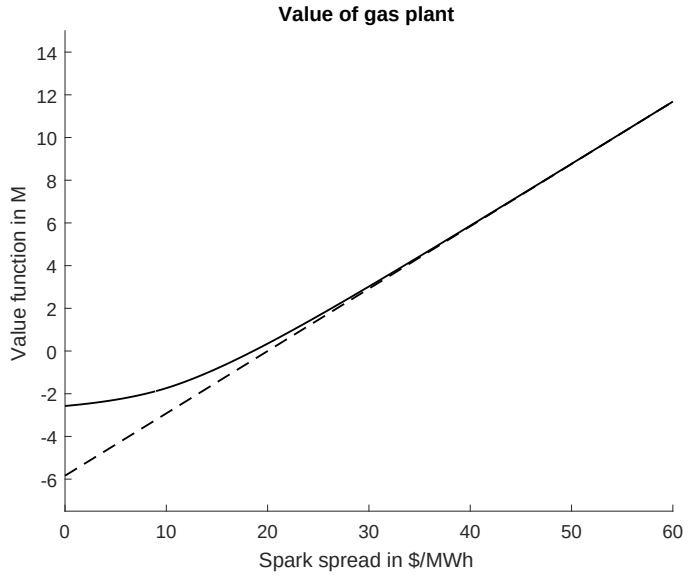

Figure 1: This figure plots the value V_1 of the gas plant in the operating state. The dashed line corresponds to the value V_{cont} of continuous operation. Parameter values can be found in Section 4.5.

for $x > 0$. It can be seen that the premium $V_1 - V_{cont}$ due to the operational flexibility and possibility of shutting down is simply $B_1 e^{\widetilde{\alpha} x}$ for $x > b_1$. It has substantial value when the spark spread X is low.

The value function V_1 converges to an affine function as the spark spread goes to infinity. Value increases when the volatility and drift of the spark spread increase, and decreases when the costs of operations and switching increase.

3. Production from renewables: wind plant

An alternative way to produce electricity is to use renewables.[2] The main alternatives are hydro, solar and wind. Our benchmark model focuses on wind power.

3.1. A model for a wind plant

The profit generated by a wind power plant depends on the price of electricity, the subsidy for generation from renewables and the cost of operating the plant. We assume that the price of electricity follows a geometric Brownian motion process under a risk-neutral measure,

$$dY_t = \mu_Y Y_t dt + \sigma_Y Y_t dZ_t, \quad Y_0 = y,$$

where Z is a standard Brownian motion positively correlated with B, and the parameters μ_Y and $\sigma_Y > 0$ represent the expected return and the return volatility, respectively. We can

[2]Nuclear is another option. As nuclear power generation entails specific safety and implementation issues, it will not be considered in this study.

rewrite $\mu_Y = r - \delta_Y$, where $\delta_Y > 0$ is an implicit yield for electricity.[3] The subsidy for clean electricity generation is a premium on top of the market price, assumed to be a constant $s > 0$. The running cost of operations is also constant $k_w > 0$. This cost mainly consists of wages and fixed costs.

The production model assumes that the wind plant can operate indefinitely and that it always operates at full capacity. Its value is the present value of profits,

$$W(y) = \mathsf{E}_y \left[\int_0^\infty e^{-rt}(s + Y_t - k_w)dt \right]$$

for $y > 0$. Straightforward computations give,

$$W(y) = \frac{1}{\delta_Y} y + \frac{s - k_w}{r}$$

for $y > 0$.

3.2. The value of wind power

The value of the wind power plant is affine in the price of electricity. It increases (decreases) linearly with the subsidy s (running cost k_w). The value decreases with the interest rate r if and only if $s - k_w > 0$.

4. Investments in power plants

4.1. An optimal timing and selection problem

An operator with a license to build a power plant can choose to build two types of production units, either using traditional fuels (gas-fired) or renewables (wind). The value of a gas-fired plant is $V_g(x) = \max\{V^0(x), V^1(x)\}$. The value of a wind plant is $W(y)$. The option to choose between the two types of plants has payoff,

$$\max\{V_g(x) - K_g, W(y) - K_w\}$$

where $K_g > 0$ and $K_w > 0$ represent the sunk costs for a gas-fired system and a wind plant, respectively. As wind plants are more expensive compared to the most efficient gas-fired plants, $K_w > K_g$.

The operator can also choose the timing τ of the investment. The value of the license to build a power plant, either gas-fired or wind-based, is therefore given by,

$$V(x, y) = \sup_{0 \le \tau \le \infty} \mathsf{E}_{x,y} \left[e^{-r\tau} \max(V_g(X_\tau) - K_g, W(Y_\tau) - K_w) \right]$$

for $x \in I\!R$ and $y > 0$. This is the value of an American option on the maximum of two assets with different strikes, i.e., a dual strike max-option. Moreover, one of the underlying asset prices, namely the price of the gas-fired plant, is itself the maximum between the two values associated with the different states of the system. A priori, the operator could decide to build when the system is in either one of the two possible states.

[3]The price of a non-storable commodity, such as electricity, can diverge from risk neutral valuation leading to the emergence of an implicit yield.

4.2. The option payoff

In order to solve the valuation problem, first note that building a gas-fired plant in an idle state, is suboptimal for the license holder. This follows from the fact that the net benefit from building the plant in that state is strictly negative. Therefore, the American dual strike max-option problem reduces to,

$$V(x,y) = \sup_{0\leq\tau\leq\infty} \mathsf{E}_{x,y}\left[e^{-r\tau}\max(V_1(X_\tau)-K_g, W(Y_\tau)-K_w)\right]$$

a more standard form. To standardize notation let $K_1 \equiv K_g$.

Second, given the value functions for V_1 and W , the dual-strike payoff becomes,

$$G(x,y) = \max\left(B_1 e^{\widetilde{\alpha}x} + \frac{x+\mu_x/r-k_1}{r} - K_1, \frac{1}{\delta_Y}y + \frac{s-k_w}{r} - K_w\right)$$

for $x > b_1$ and $y > 0$ as the operator should not enter into the gas-fired plant when $x \leq b_1$. It is also clear that the operator should not enter into the wind technology when $y \leq \delta_Y(K_w - \frac{s-k_w}{r})$ as the payoff is negative.

We define an increasing function,

$$\widehat{y}(x) = \delta_Y\left(B_1 e^{\widetilde{\alpha}x} + \frac{x+\mu_x/r-k_1}{r} - K_1 - \frac{s-k_w}{r} + K_w\right)$$

for $x > b_1$ and its inverse $\widehat{x}(y)$ for $y > \widehat{y}(b_1)$, i.e.,

$$\widehat{x}(\widehat{y}(x)) = x$$

for $x > b_1$. It is then clear that,

$$G(x,y) = G_1(x) := B_1 e^{\widetilde{\alpha}x} + \frac{x+\mu_x/r-k_1}{r} - K_1$$

for $x > b_1$ and $y \leq \widehat{y}(x)$ and,

$$G(x,y) = G_2(y) := \frac{1}{\delta_Y}y + \frac{s-k_w}{r} - K_w$$

for $x > b_1$ and $y > \widehat{y}(x)$ or any $x \leq b_1$.

4.3. Optimal investment in power generation

1. *Exercise region.* We now characterize the optimal investment strategy for the operator. First, let us define the investment ($\mathcal{D}$) and continuation ($\mathcal{C}$) regions,

$$\mathcal{D} = \{(x,y) \in I\!R \times (0,\infty) : V(x,y) = G(x,y)\}$$
$$\mathcal{C} = \{(x,y) \in I\!R \times (0,\infty) : V(x,y) > G(x,y)\}$$

and, as suggested by the analysis in Section 4.2, split the investment region $\mathcal{D}$ into two parts,

$$\mathcal{D}_g = \{(x,y) \in \mathcal{D} : G(x,y) = G_1(x)\} \quad \text{and} \quad \mathcal{D}_w = \{(x,y) \in \mathcal{D} : G(x,y) = G_2(y)\}.$$

In the region $\mathcal{D}_g$, it is optimal to invest in the gas-fired plant; in $\mathcal{D}_w$ the wind plant investment is optimal. As the payoff G is a continuous function, the optimal investment timing rule is given by $\tau_* = \inf\{t \geq 0 : (X_t, Y_t) \in \mathcal{D}\}$.

To gain further insights into the structure of the investment region, we exploit the local time-space formula (see Peskir (2005)), to obtain,

$$
\begin{aligned}
(4.1) \qquad & \mathsf{E}_{x,y}\left[e^{-r\tau}\max(V_1(X_\tau)-K_v, W(Y_\tau)-K_w)\right] \\
&= G(x,y) + \mathsf{E}_{x,y}\left[\int_0^\tau e^{-rt} H_1(X_t) I(G(X_t,Y_t)=G_1(X_t))dt\right] \\
&\quad + \mathsf{E}_{x,y}\left[\int_0^\tau e^{-rt} H_2(Y_t) I(G(X_t,Y_t)=G_2(Y_t))dt\right] \\
&\quad + \frac{1}{2\delta_Y}\mathsf{E}_{x,y}\left[\int_0^\tau e^{-rt} d\ell_t\right]
\end{aligned}
$$

for $(x,y) \in I\!R \times (0,\infty)$ and any stopping time τ where ℓ is the local time process that Y spends at $\widehat{y}$, and H_1 and H_2 represent the local gains of waiting to invest into the gas-fired and wind technologies, respectively, which are defined as,

$$
\begin{aligned}
H_1(x) &= I\!L_X G_1(x) - rG_1(x) = -x + k_1 + rK_1 \\
H_2(y) &= I\!L_Y G_2(y) - rG_2(y) = -y - (s-k_w) + rK_w
\end{aligned}
$$

for $(x,y) \in I\!R \times (0,\infty)$. As we maximize the left-hand side of (4.1) over all stopping times, it is clear that the investor should not enter into the gas-fired technology when $X_t < k_1 + rK_1$ as $H_1(X_t) > 0$ and into the wind plant when $Y_t < rK_w - (s-k_w)$ as $H_2(Y_t) > 0$. Therefore, $b_X(y) \geq k_1 + rK_1$ for $y > 0$ and $b_Y(x) \geq rK_w - (s-k_w)$ for $x \in I\!R$. Also, (4.1) shows that the operator should not invest at all along the curve $\widehat{y}$, i.e., when $Y_t = \widehat{y}(X_t)$, as the local time term dominates the two other terms in dt. In other words, $\{(x,y) \in I\!R \times (0,\infty) : x > b_1, y = \widehat{y}(x)\} \in \mathcal{C}$.

2. The next theorem describes the structure of the immediate investment set $\mathcal{D}$. Figure 2 illustrates its shape.

Theorem 4.1. *There exist two boundaries $b_X : (0,\infty) \to I\!R$ and $b_Y : I\!R \to (0,\infty)$ such that (i) The sets $\mathcal{C}$ and $\mathcal{D}$ are given by,*

$$
\begin{aligned}
\mathcal{D}_g &= \{(x,y) \in I\!R \times (0,\infty) : x \geq b_X(y)\} \\
\mathcal{D}_w &= \{(x,y) \in I\!R \times (0,\infty) : y \geq b_Y(x)\} \\
\mathcal{C} &= \{(x,y) \in I\!R \times (0,\infty) : y < b_Y(x) \;\&\; x < b_X(y)\}.
\end{aligned}
$$

(ii) Both boundaries b_X and b_Y are convex (thus continuous) and increasing functions on $(0,\infty)$ and $I\!R$.
(iii) The limiting values are $b_X(0+) = b_X^g$ and $b_Y(-\infty) = b_Y^w$, where b_X^g and b_Y^w are the optimal thresholds of standard timing problems for gas-fired and wind plants, respectively,

$$
\sup_{0\leq\tau\leq\infty} \mathsf{E}_x\left[e^{-r\tau}(V_g(X_\tau)-K_g)\right], \qquad \textit{and} \qquad \sup_{0\leq\tau\leq\infty} \mathsf{E}_y\left[e^{-r\tau}(W(Y_\tau)-K_w)\right]
$$

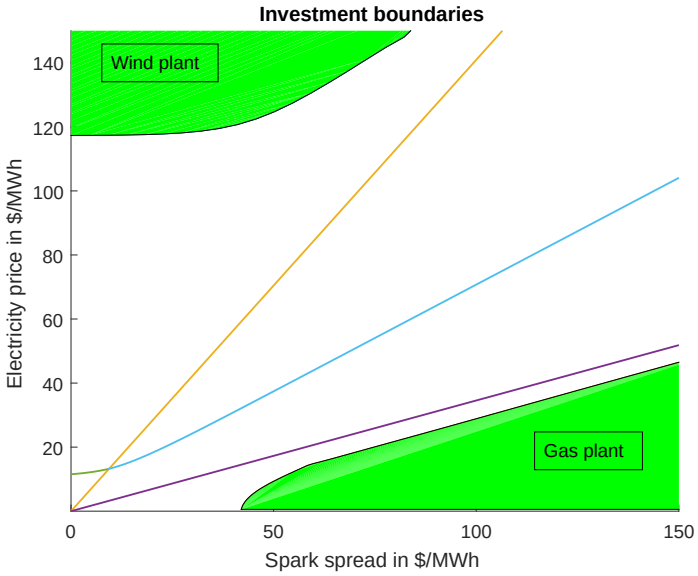

Figure 2: This figure shows the immediate investment region $\mathcal{D} = \mathcal{D}_g \cup \mathcal{D}_w$. Immediate investment in the gas (wind) plant is optimal in $\mathcal{D}_g$ (in $\mathcal{D}_w$). The straight lines are the edges of the asymptotic no-investment cone. The curve corresponds to $\widehat{y}(x)$, where the two projects have the same value.

for $x \in I\!R$ *and* $y > 0$.
(iv) The following inequalities hold: $b_X(y) > \widehat{x}(y)$ *for* $y > \widehat{y}(b_1)$ *and* $b_X(y) > b_X^g$ *for* $y > 0$ *;* $b_Y(x) > \widehat{y}(x)$ *for* $x > b_1$ *and* $b_Y(x) > b_Y^w$ *for* $x \in I\!R$.

Property (i) indicates that the operator should invest in the gas-fired technology when the spark spread x exceeds the boundary $b_X(y)$ and in the wind plant when the price of electricity y exceeds the boundary $b_Y(x)$. Each boundary depends on an underlying state variable: the threshold for investment in the gas-fired (resp. wind) plant depends on the price of electricity (resp. spark spread). Moreover, the investment events determined by the boundaries are mutually exclusive: the boundaries do not cross and the sets $\mathcal{D}_g$ and $\mathcal{D}_w$ do not intersect (see Figure 2 for illustration). Convexity of the boundaries in Property (ii) ensures that the exercise regions are convex as well. Thus, if investment in a given technology is optimal at two point $(x_j, y_j), j = 1, 2$. it will also be optimal at any convex combination $\left(x^\lambda, y^\lambda\right) = \lambda(x_1, y_1) + (1-\lambda)(x_2, y_2)$ for $\lambda \in [0, 1]$. Property (iii) establishes a relation between the boundaries $b_X(y), b_Y(x)$ and those when the operator considers an investment in a specific technology. It shows that these boundaries differ, except in extreme circumstances where the spark spread goes to $-\infty$, in which case the license to invest becomes an option to build a wind plant, or where the price of electricity approaches 0 and the license collapses to an option to invest in the gas-fired technology. When both alternatives are considered, Property (iv) elaborates and shows that the thresholds of these single asset options are in fact lower bounds for the investment boundaries in the two asset problem. The selection option adds value to the operator's license ensuring that it is optimal to delay investments relative to the single technology case. Property (iv) also highlights a striking aspect, namely the fact

that immediate investment in any technology is always suboptimal along the curve $\widehat{y}(x)$ (or it inverse $\widehat{x}(y)$). This is true irrespective of the size of the spark spread or the price of electricity. Hence, even when the options to invest in single technologies are deep in the money, it may still be optimal to wait before investing when technological choices are factored in. The extent of these optimal delays and the size of the premium generated by waiting are quantified in Section 4.5.

2. *Integral equations.* Theorem 4.2 is the main result of this section. It gives a characterization of the optimal investment strategy.

Theorem 4.2. *The optimal investment boundaries solve the pair of coupled integral equations,*

$$G_1(b_X(y)) = \pi(b_X(y), y; b_X, b_Y) \tag{4.2}$$

$$G_2(b_Y(x)) = \pi(x, b_Y(x); b_X, b_Y) \tag{4.3}$$

for $y > 0$ *and* $x \in \mathbb{R}$ *, where* $\pi(x, y; b_X, b_Y)$ *represents the early investment premium (EIP) defined as,*

$$\pi(x, y; b_X, b_Y) = \pi_1(x, y; b_X) + \pi_2(x, y; b_Y) \tag{4.4}$$

$$\pi_1(x, y; b_X) = -\mathsf{E}_{x,y}\left[\int_0^\infty e^{-rt} H_1(X_t) I(X_t \geq b_X(Y_t)) dt\right] \tag{4.5}$$

$$\pi_2(x, y; b_Y) = -\mathsf{E}_{x,y}\left[\int_0^\infty e^{-rt} H_2(Y_t) I(Y_t \geq b_Y(X_t)) dt\right]. \tag{4.6}$$

Explicit expressions for the premium components are in Lemma 7.1 in the Appendix.

Theorem 4.2 shows that the boundaries solve a system of coupled integral equations. These equations derive from the Early Investment Premium (EIP) representation of the value of the license held by the operator, which is described in Section 4.4. As there are two subregions, the EIP premium $\pi(x, y; b_X, b_Y)$ has two components corresponding respectively to the value of investing when the gas-fired technology is optimal ($\pi_1(x, y; b_X)$) and when the wind technology is optimal ($\pi_2(x, y; b_Y)$). Because each premium component depends on its corresponding boundary, the equations are coupled. Hence, the boundary b_X depends on b_Y , and conversely.

This characterization of the optimal investment boundaries is reminiscent of the characterization typically obtained for the exercise boundaries of American max-call options (e.g., Broadie and Detemple (1997)). Although the structural form of the two systems appears similar, they differ in several respects. First, in (4.2)-(4.3) there is no term relating to a European option component. This follows from the assumption that the license to operate is infinitely lived. In this case, the residual value at the terminal date vanishes. Second, the equations do not have a recursive structure in time or space. The absence of recursivity with respect to time comes from the infinite horizon nature of the problem. The absence of recursivity in space is due to the fact that boundaries are integrated over their respective domains in the premium. As a result the integral equations are not of the typical Volterra type as in standard American option pricing problems. Third, the investment payoffs involve a nonlinear, exponential-affine function of an underlying variable. In contrast, the standard max-call has a linear payoff in the exercise region. Finally, underlying variables evolve according to a geometric Brownian motion

and an arithmetic Brownian motion. This mixture of processes invalidates scaling properties found in standard models based on geometric Brownian motion.

3. *Asymptotic behavior of the boundaries.* The system of coupled integral equations (4.2)-(4.3) can, in principle, be used to compute the optimal investment boundaries. One of the difficulties in implementing an algorithm based on these equations is the unboundedness of the domains over which boundaries are defined. The next result, which describes the asymptotic behavior of the boundaries, helps to address this issue. It shows that boundaries have linear growth and provides their exact slopes. We extract these slopes from the system of integral equations (4.2)-(4.3), and are not aware of any other method to achieve this. This shows another advantage and highlights the informational content of these equations.

Proposition 4.3. *The following identities hold,*

$$\lim_{y\uparrow+\infty}\frac{b_X(y)}{y}=b_X^\infty \qquad \textit{and} \qquad \lim_{x\uparrow+\infty}\frac{b_Y(x)}{x}=b_Y^\infty$$

where the slopes b_X^∞ *and* b_Y^∞ *can be computed, respectively, as*

$$b_X^\infty=\frac{\int_0^\infty e^{-\delta_Y t}\int_{-\infty}^\infty \varphi(z_1)\Phi\left(-\frac{\frac{1}{\sigma_Y\sqrt{t}}\left(\log(b^\infty)-\left(\mu_Y+\frac{1}{2}\sigma_Y^2\right)t\right)-\rho z_2}{\sqrt{1-\rho^2}}\right)dz_1\,dt}{1/r-\int_0^\infty e^{-rt}\int_{-\infty}^\infty \varphi(z_1)I\left(\left(\mu_Y-\frac{1}{2}\sigma_Y^2\right)t+\sigma_Y\sqrt{t}z_1<0\right)dz_1\,dt}$$

$$b_Y^\infty=\frac{\int_0^\infty e^{-rt}\int_{-\infty}^\infty \varphi(z_1)I\left(b^\infty\exp\left\{\left(\mu_Y-\frac{1}{2}\sigma_Y^2\right)t+\sigma_Y\sqrt{t}z_1\right\}<1\right)dz_1\,dt}{1/\delta_Y-\int_0^\infty e^{-\delta_Y t}\int_{-\infty}^\infty \varphi(z_2)\Phi\left(\frac{1}{\sqrt{1-\rho^2}}\left((\mu_Y/\sigma_Y+\sigma_Y/2)\sqrt{t}+\rho z_2\right)\right)dz_2\,dt}$$

and where the product of the slopes $b^\infty=b_X^\infty b_Y^\infty$ *is the unique solution to*

$$\begin{aligned}(4.7)\qquad b^\infty=&\frac{\int_0^\infty e^{-\delta_Y t}\int_{-\infty}^\infty \varphi(z_1)\Phi\left(-\frac{\frac{1}{\sigma_Y\sqrt{t}}\left(\log(b^\infty)-\left(\mu_Y+\frac{1}{2}\sigma_Y^2\right)t\right)-\rho z_2}{\sqrt{1-\rho^2}}\right)dz_1\,dt}{1/r-\int_0^\infty e^{-rt}\int_{-\infty}^\infty \varphi(z_1)I\left(\left(\mu_Y-\frac{1}{2}\sigma_Y^2\right)t+\sigma_Y\sqrt{t}z_1<0\right)dz_1\,dt}\\ &\times\frac{\int_0^\infty e^{-rt}\int_{-\infty}^\infty \varphi(z_1)I\left(b^\infty\exp\left\{\left(\mu_Y-\frac{1}{2}\sigma_Y^2\right)t+\sigma_Y\sqrt{t}z_1\right\}<1\right)dz_1\,dt}{1/\delta_Y-\int_0^\infty e^{-\delta_Y t}\int_{-\infty}^\infty \varphi(z_2)\Phi\left(\frac{1}{\sqrt{1-\rho^2}}\left((\mu_Y/\sigma_Y+\sigma_Y/2)\sqrt{t}+\rho z_2\right)\right)dz_2\,dt}.\end{aligned}$$

In these formulas, φ *and* Φ *are the standard normal cdf and pdf, respectively.*

We also have that $b_X^\infty\cdot y\le b_X(y)$ *for any* $y>0$ *and* $b_Y^\infty\cdot x\le b_Y(x)$ *for any* $x\in\mathbb{R}$.

4. *Algorithm.* Having obtained the system of integral equations, the expression for the early investment premium π and the asymptotic behavior of the boundaries, we now propose a numerical algorithm to compute the pair of boundaries (b_X,b_Y). In this paragraph, we describe the main idea of the procedure; details are in the Appendix. We note that this approach can be extended to other perpetual multidimensional timing problems.

As noted above, the integral equations are not of Volterra type and this is in contrast to standard situations in American option problems where the time-dependent boundaries are

solutions to recursive integral equations, which can be solved by backward induction. In our case, the equations are of Fredholm type, i.e., to extract $b_Y(x)$ we need to know the values of $b_Y(\widetilde{x})$ for both $\widetilde{x} < x$ and $\widetilde{x} > x$. Thus, we do not have recursive induction in x. However, we make use of the following iterative procedure. Let us choose some initial curves $(b_X^0(y), b_Y^0(x))$ for $x \in I\!R$ and $y > 0$, and then, recursively, define $b_X^n(y)$ and $b_Y^n(x)$ as solutions to the algebraic equations,

$$G_1(b_X^n(y)) = \pi(b_X^{n-1}(y), y; b_X^{n-1}, b_Y^{n-1}) \tag{4.8}$$

$$G_2(b_Y^n(x)) = \pi(x, b_Y^{n-1}(x); b_X^{n-1}, b_Y^{n-1}) \tag{4.9}$$

for $y > 0$, $x \in I\!R$ and $n \geq 1$. The intuition behind this recursive approach is that if the sequence of boundaries (b_X^n, b_Y^n) converges as $n \to \infty$, the equations in the limit correspond to the integral equations satisfied by the exercise boundaries (b_X, b_Y).

The advantage of this method is that, at step n, the right-hand sides are fixed and do not depend on b_X^n and b_Y^n, and the left-hand sides are increasing functions of $b_X^n(y)$ and $b_Y^n(x)$, respectively. Thus, there are unique solutions to both equations. In fact, as G_2 is affine in y, we have an explicit expression for $b_Y^n(x)$. The same is not true for G_1, because of its nonlinear structure, so that we have to solve that algebraic equation.

Let us now describe the natural candidate for the initial values of the sequence, namely (b_X^0, b_Y^0). As we identified lower bounds for (b_X, b_Y), we define initial values as follows,

$$b_X^0(y) = \begin{cases} b_X^g, \ y < b_X^g/b_X^\infty \\ b_X^\infty y, \ y \geq b_X^g/b_X^\infty \end{cases} \quad \text{and} \quad b_Y^0(x) = \begin{cases} b_Y^w, \ x < b_Y^w/b_Y^\infty \\ b_Y^\infty x, \ x \geq b_Y^w/b_Y^\infty. \end{cases}$$

We then iterate for $n = 1, 2, ...$ until the variation $\left(b_X^n(y) - b_X^{n-1}(y), b_Y^n(x) - b_Y^{n-1}(x)\right)$ falls below a predetermined tolerance threshold. The complete details of the algorithm such as truncation, discretization, interpolation and extrapolation of the state space and boundaries are given in the Appendix.

4.4. The value of investing in power generation

Having recovered the optimal investment boundaries, we can now determine the value of the operator's license.

Proposition 4.4. *(Early Investment Premium representation) The value of the option to invest in power generation from the best of a gas-fired plant or a wind plant is,*

$$V(x, y) = \pi(x, y; b_X, b_Y)$$

for $y > 0$ and $x \in I\!R$, where the function $\pi(\cdot, \cdot, \cdot, \cdot)$ is the EIP. The EIP is parametrized by the boundaries (b_X, b_Y) solving (4.2)-(4.3).

Proposition 4.4 shows that the value of the license to invest in either of the two technologies, hence the best of the two technologies, stems entirely from the early investment premium. This premium is the present value of the cumulative instantaneous gains from investing in the wind plant when such a choice is optimal and those from investing in the gas-fired plant when the

latter is optimal. As explained previously, there is no European-style component due to the perpetual nature of the license.

An immediate application of Proposition 4.4 gives the premium generated by the option to invest in the alternative wind technology, instead of the traditional gas-fired technology. Indeed, for $y = 0$, the function $V(x, 0)$ represents the value of a license to invest in power production by building a gas-fired plant. For $y > 0$, the function $V(x, y)$ gives the value of a license to invest in the best of the two technologies. The increment,

$$V(x, y) - V(x, 0)$$

is the premium associated with the option to choose the alternative production technology. It captures to value created by the option to produce from a renewable source, i.e., wind in our model, as opposed to a traditional fuel such as gas.

4.5. Investing in power generation: numerical results

We now perform a numerical study to examine the investment decision and the resulting value created. An important goal is to understand the premium associated with the use of renewables.

1. *Model calibration.* Parameter values under the risk neutral measure are described in Table 1. The interest rate is $r = 0.03$. For the electricity price Y, which follows a geometric Brownian motion, the drift is $\mu_Y = 0.02$ and the volatility $\sigma_Y = 0.3$. For the spark spread X, which is arithmetic Brownian motion, we set $\mu_X = 0$ and $\sigma_X = 2$. The correlation between the two processes is $\rho = 0.3$. For reference, typical values of wholesale electricity prices were in the range $\$10 - \$120$ per MWh during the period 2016-2017. Typical values of the spark spread, calculated using a standard benchmark heat rate of 7 Btu/MWh, fluctuated between $-\$10$ and $\$100$ per MWh. Parameter values are comparable to estimates reported in Lucia and Schwartz (2003), Maribu, Galli and Armstrong (2007) and Boomsma, Meade and Fleten (2012).

	spark spread $z = x$	electricity price $z = y$
Drift μ_z	0	0.02
Volatility σ_z	2	0.3

Table 1: Parameter values.

Figure 3 shows typical trajectories for X and Y. The spark spread is less volatile ($\sigma_X = 2$) than the electricity price ($Y \times \sigma_Y = 12$) reflecting the fact that the price of natural gas is less volatile and that the spark spread is the difference between the two prices adjusted by the heat rate. The drift of the spark spread is set at zero due to the absence of a long term trend in the time series.[4]

[4]For numerical computations, dollars per MWh are converted to millions of dollars per MWy (megawatt /year). The adjustment factor is $365 \times 24/1000000 = 0.00876$. Hence 1 \$/MWh equals 0.00876 M per MWy. This factor applies to prices and to the coefficients of the spark spread process.

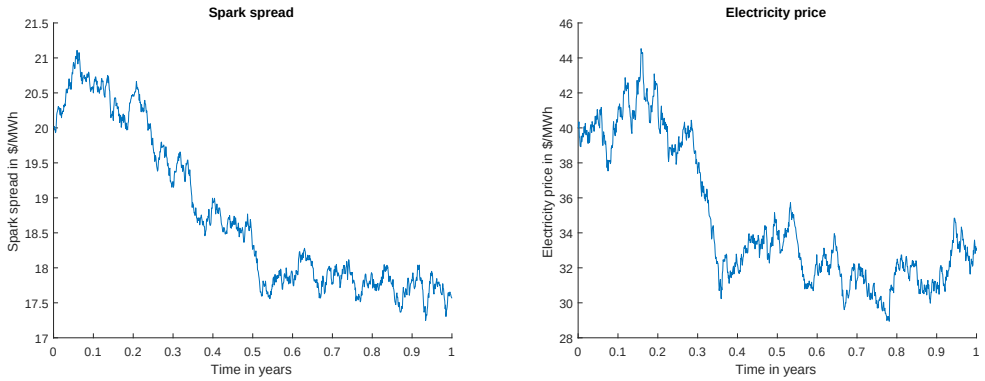

Figure 3: This figure shows typical trajectories for the spark spread X (left) and the electricity price Y (right).

The costs of operations for the gas-fired plant are $k_0 = 10$ and $k_1 = 20$ per MWh. Switching costs are set at $c_0 = 0.002$ M and $c_1 = 0.001$ M. These costs capture switches between full capacity operation and idleness for extended periods of time. Costs of restarts increase significantly after a few days due to equipment failure. The running cost for the wind plant is $k_w = 45$ per MWh and we assume that the subsidy rate $s = 23$ per MWh.

The cost per MW of a wind turbine varies between 1.3 M and 2.2 M. For natural gas power plants, typical construction costs vary between 0.7 M and 2 M per MW depending on the type of technology deployed. We use the averages for investment costs, namely 1.75 M and 1.35 M, with a correction for future replacement costs.[5] This gives adjusted investment costs of $K_w = 5.3$ and $K_g = 4.1$.

2. *Investment decision.* Figure 2 illustrates the structure of the immediate investment region, along with the asymptotic cone with slopes b_X^∞, b_Y^∞ and the curve $\widehat{y}(x)$ along which the two projects have the same value. Figure 4 shows the impact of the cost of investment in the wind plant. As the cost decreases, the payoff from an investment in the wind project increases, thereby increasing the value of the timing option. The investment boundaries therefore decrease and the immediate investment region expands. Increases in the volatilities of the spark spread and/or of the electricity price have the opposite effect as shown in the Figure 5. This follows from the convexity of the value of the gas-fired plant and the convexity of the $\max\{\cdot,\cdot\}$ function.

3. *The value of waiting.* Figure 6 plots the value of waiting to invest along the curve $\widehat{y}(x)$, as a function of the spark spread x . We already know that immediate investment is suboptimal, hence the value of waiting is positive, along this curve because the underlying projects have the same values. What the figure reveals is that the value of waiting actually increases as the spark spread increases, beyond some threshold. This shows that the incentive to wait eventually grows, even when the underlying projects become more valuable. As the spark spread increases, the potential gain in the best of the two projects increases, for a given innovation in (B, Z) . This follows from the multiplicative structure of the electricity price (GBMP) and the fact that the max payoff increases when either of the two project values

[5]We assume that costs grow at 1% per year and that equipment needs to be replaced every 20 years.

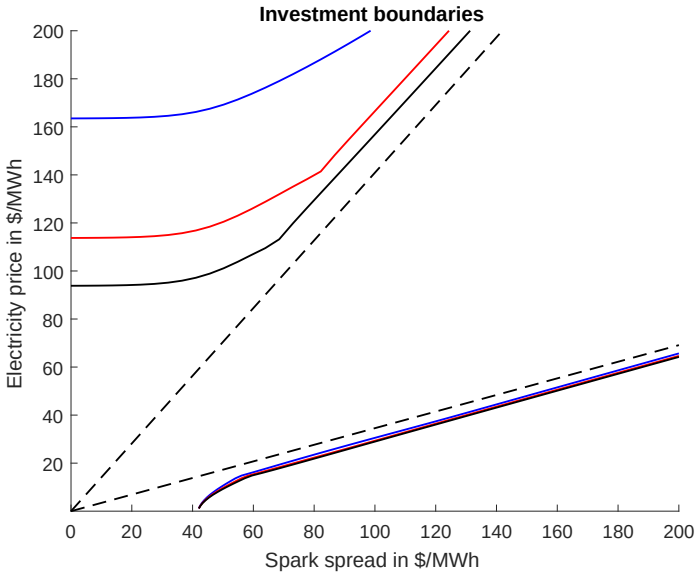

Figure 4: This figure shows the impact of the cost of investment K_w in the wind plant. Black lines correspond to investment boundaries for $K_w = 3$, red lines for $K_w = 5$ and blue lines for $K_w = 10$. Dashed lines are the edges of the asymptotic no-investment cone.

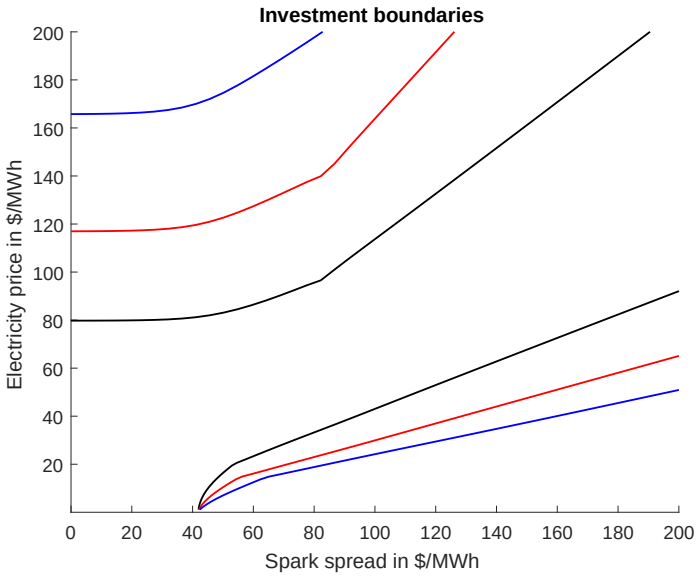

Figure 5: This figure shows the impact of the volatility σ_Y of the electricity price. Black lines correspond to investment boundaries for $\sigma_Y = 0.2$, red lines for $\sigma_Y = 0.3$ and blue lines for $\sigma_Y = 0.4$.

increases. A larger response of the electricity price triggers a greater variation in the value of the gas plant. For small changes, the likelihood of an increase in the max-payoff if the operator waits is close to 75%. The gain in this event remains the same or increases as the spark spread

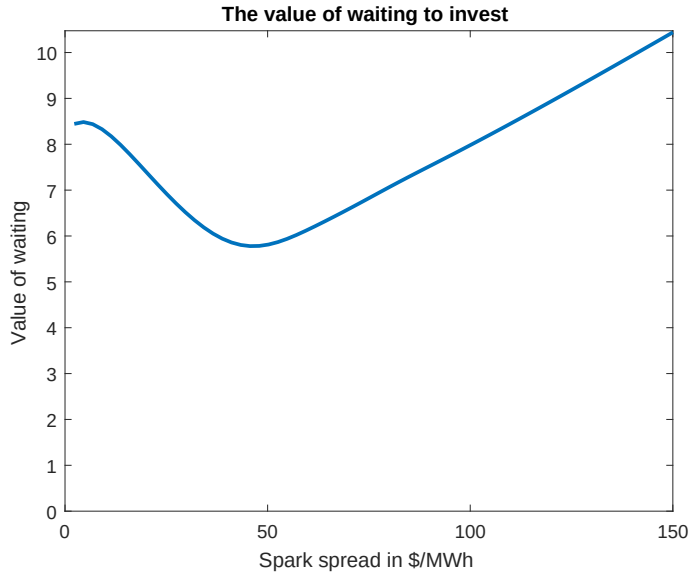

Figure 6: This figure plots the value of waiting to invest along the curve $\widehat{y}(x)$, as a function of the spark spread x .

increases. The likelihood of a decrease is about 25% and the loss depends on which of the two projects values decreases more. Hence the loss in this event either stays the same or increases. As the first event is significantly more likely, it dominates and leads to an overall increase in the value of waiting, as displayed in the graph.

4. *The value of renewables.* Figures 7 and 8 illustrate the benefits associated with a potential investment in the wind farm. Figure 7 shows that the value of the license to invest in the best of the two technologies $V(x, y)$ can increase by a factor of 10 or more, relative to the value of a license to invest in a gas plant, when the spark spread is sufficiently low. The wind premium $V(x, y) - V(x, 0)$ is graphed in Figure 8 for constant values of the electricity price. This premium is substantial. It decays slowly as the spark spread increases to eventually vanish when investment in the gas-fired plant becomes optimal. The premium remains positive and significant, even when the spark spread becomes large.

5. *Renewables subsidies.* Figure 9 shows the impact of subsidies to renewables power generation. As subsidies increase, the value of the wind plant increases and so does the incentive to invest early. As seen from the graph, the impact on the boundary for investment in the wind plant is substantial.

5. Extension

5.1. Extension A: mean reversion

This section develops an extension of the base model that incorporates mean reversion in the spark spread process. We model the spark spread as the mean-reverting Gaussian process, i.e.

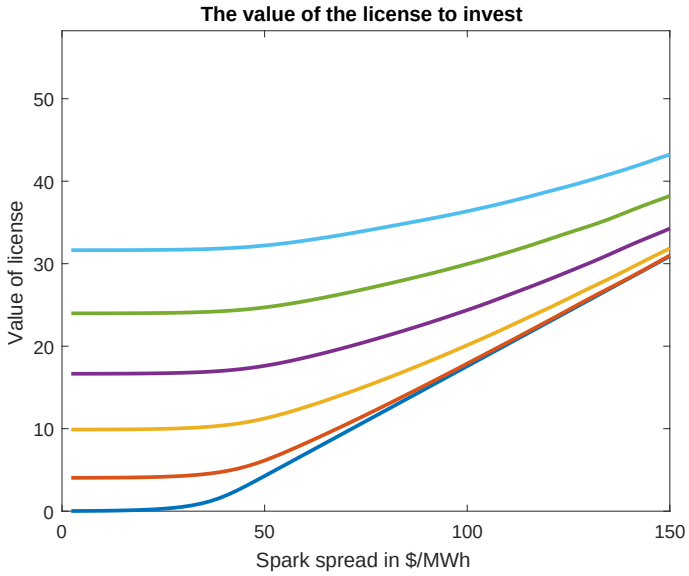

Figure 7: This figure shows that the value of the license $V(x, y)$ to invest in the best of the two technologies as a function of the spark spread x for fixed electricity price y \$/MWh. Dark blue line: $y = 0$; red line: $y = 20$; orange line: $y = 40$; purple line: $y = 60$; green line: $y = 80$; light blue line: $y = 100$.

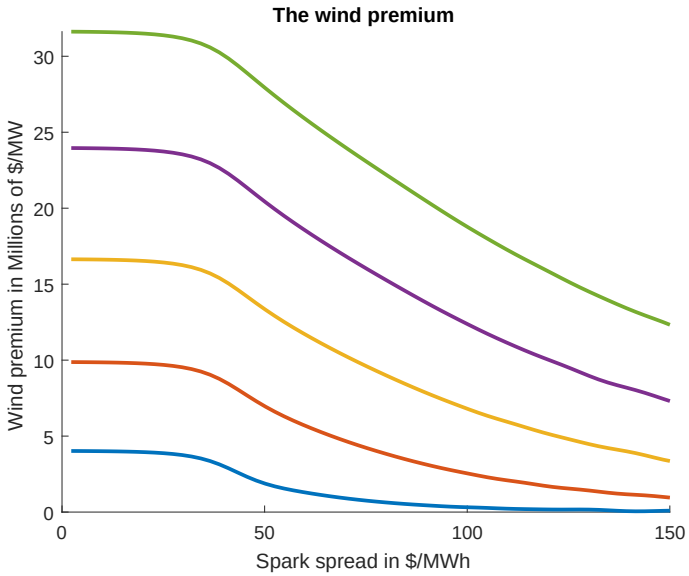

Figure 8: This figure plots the wind premium $V(x, y) - V(x, 0)$ for constant values of the electricity price y \$/MWh. Dark blue line: $y = 0$; red line: $y = 20$; orange line: $y = 40$; purple line: $y = 60$; green line: $y = 80$.

Ornstein-Uhlenbeck (OU) process under the risk-neutral measure,

$$dX_t = \mu_X(\theta_X - X_t)dt + \sigma_X dB_t, \quad X_0 = x,$$

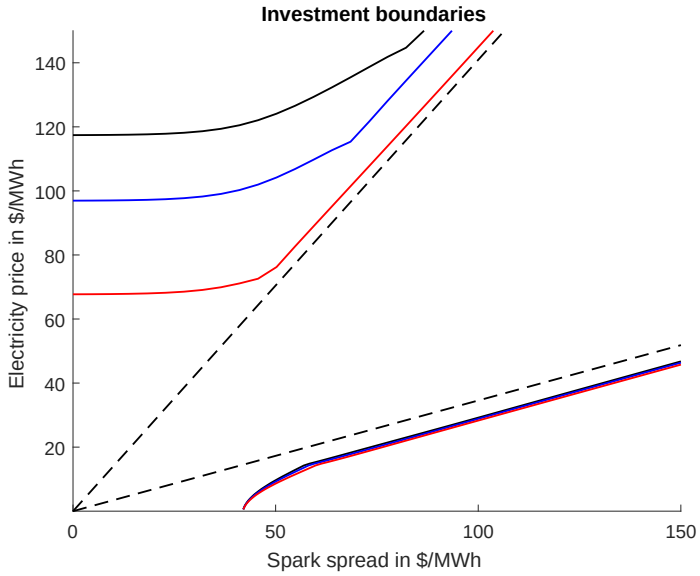

Figure 9: This figure shows the impact of the subsidy rate s. Black lines correspond to investment boundaries for $s = 23$, blue lines for $s = 30$ and red lines for $s = 40$.

where B is a standard Brownian motion, and the constant parameters μ_X, θ_X and $\sigma_X > 0$ represent the mean-reversion speed, long-run level and volatility, respectively. We assume that B is correlated with Z (Brownian shocks in the electricity price) with correlation $\rho \in [0, 1]$. We still impose the GBMP model for the electricity price Y.

1. As under the arithmetic Brownian motion model, the operator of the plant has the possibility of switching back and forth between the two states of operation. The optimal switching decisions are determined by two thresholds, $b_0 > b_1$. When the plant is idle, it becomes optimal to turn the system on when X_t hits b_0 from below. When it operates, it becomes optimal to cease production when X_t reaches b_1 from above.

For the OU model, the value of idling satisfies the following ODE,

$$\frac{\sigma_X^2}{2} V_0''(x) + \mu_X(\theta_X - x)V_0'(x) - rV_0(x) - k_0 = 0$$

for $x < b_0$. The general solution to this ODE is given by,

$$V_0(x) = A_0 F(x) + B_0 \widetilde{F}(x) - \frac{k_0}{r}$$

where the function F and $\widetilde{F}$ are,

$$F(x) = \int_0^\infty u^{\frac{r}{\mu_X}-1} e^{\sqrt{2\mu_X/\sigma_X^2}(x-\theta_X)u - \frac{u^2}{2}} du$$
$$\widetilde{F}(x) = \int_0^\infty u^{\frac{r}{\mu_X}-1} e^{\sqrt{2\mu_X/\sigma_X^2}(\theta_X-x)u - \frac{u^2}{2}} du$$

for $x \in I\!R$. We observe that both F and $\widetilde{F}$ are strictly positive and convex, and that they are, respectively, strictly increasing and decreasing. As V_0 is bounded, we have that $B_0 = 0$ and thus,

$$V_0(x) = A_0 F(x) - \frac{k_0}{r}$$

for $x < b_0$.

Likewise, the value of operating satisfies,

$$\frac{\sigma_X^2}{2} V_1''(x) + \mu_X(\theta_X - x)V_1'(x) - rV_1(x) + x - k_1 = 0$$

for $x > b_1$. The solution to this ODE is given by,

$$V_1(x) = B_1 \widetilde{F}(x) + \frac{1}{\mu_X + r} x + \frac{1}{r}\left(\frac{\mu_X \theta_X}{\mu_X + r} - k_1\right)$$

as V_1 is bounded and where B_1 is some constant.

Given the above expressions for the value functions and using the continuous and smooth pasting conditions at b_0 and b_1, we derive to the system of four algebraic equations with four unknown variables (b_0, b_1, A_0, B_1),

$$A_0 F(b_0) - \frac{k_0}{r} = B_1 \widetilde{F}(b_0) + \frac{1}{\mu_X + r} b_0 + \frac{1}{r}\left(\frac{\mu_X \theta_X}{\mu_X + r} - k_1\right) - c_0 \tag{5.1}$$

$$A_0 F'(b_0) = B_1 \widetilde{F}'(b_0) + \frac{1}{\mu_X + r} \tag{5.2}$$

$$A_0 F(b_1) - \frac{k_0}{r} - c_1 = B_1 \widetilde{F}(b_1) + \frac{1}{\mu_X + r} b_1 + \frac{1}{r}\left(\frac{\mu_X \theta_X}{\mu_X + r} - k_1\right) \tag{5.3}$$

$$A_0 F'(b_1) = B_1 \widetilde{F}'(b_1) + \frac{1}{\mu_X + r}. \tag{5.4}$$

Clearly, this system has a unique solution and can be solved numerically. The standard verification arguments shows that the solution to this system provides the value functions and optimal operation rules.

2. Now we turn to the selection problem.

$$V(x, y) = \sup_{0 \le \tau \le \infty} \mathsf{E}_{x,y}\left[e^{-r\tau} \max(V_1(X_\tau) - K_1, W(Y_\tau) - K_w)\right]$$

for $x \in I\!R$ and $y > 0$. As before we define the dual-strike payoff

$$G(x, y) = \max\left(B_1 \widetilde{F}(x) + \frac{1}{\mu_X + r} x + \frac{1}{r}\left(\frac{\mu_X \theta_X}{\mu_X + r} - k_1\right) - K_1, \frac{1}{\delta_Y} y + \frac{s - k_w}{r} - K_w\right)$$

for $x > b_1$ and $y > 0$ as the operator should not enter into the gas-fired plant when $x \le b_1$. As in the ABM model, we define an increasing function,

$$\widehat{y}(x) = \delta_Y\left(B_1 \widetilde{F}(x) + \frac{1}{\mu_X + r} x + \frac{1}{r}\left(\frac{\mu_X \theta_X}{\mu_X + r} - k_1\right) - K_1 - \frac{s - k_w}{r} + K_w\right)$$

for $x > b_1$ and its inverse $\widehat{x}(y)$ for $y > \widehat{y}(b_1)$.

The solution to the operator's problem is similar to the one in Section 4.3. The differences are that the payoff takes the adjusted form,

$$G_1(x) = B_1\widetilde{F}(x) + \frac{1}{\mu_X + r}x + \frac{1}{r}\left(\frac{\mu_X\theta_X}{\mu_X + r} - k_1\right) - K_1$$

and that the marginal distribution of

$$X_t \sim N\left(x\,e^{-\mu_X t} + \theta_X(1 - e^{-\mu_X t}), \frac{\sigma_X^2}{2\mu_X}(1 - e^{-2\mu_X t})\right)$$

has still Gaussian law but with modified mean and variance. We recall that for the ABM model we have that $X_t \sim N(x + \mu_X t, \sigma_X^2 t)$. The function H_1, which represents the local gains of waiting to invest into the gas-fired plant, has the same form as before,

$$H_1(x) = -x + k_1 + rK_1.$$

Theorem 4.1 is still valid for the OU model, thus we have two exercise boundaries b_X and b_Y, which can be determined as the solution to the system of coupled integral equations,

$$G_1(b_X(y)) = \pi(b_X(y), y; b_X, b_Y) \tag{5.5}$$

$$G_2(b_Y(x)) = \pi(x, b_Y(x); b_X, b_Y) \tag{5.6}$$

for $y > 0$ and $x \in I\!R$, where $\pi(x, y; b_X, b_Y)$ represents the early investment premium (EIP) and is defined in the same way as in Section 4.3,

$$\pi(x, y; b_X, b_Y) = \pi_1(x, y; b_X) + \pi_2(x, y; b_Y) \tag{5.7}$$

$$\pi_1(x, y; b_X) = -\mathsf{E}_{x,y}\left[\int_0^\infty e^{-rt}H_1(X_t)I(X_t \geq b_X(Y_t))dt\right] \tag{5.8}$$

$$\pi_2(x, y; b_Y) = -\mathsf{E}_{x,y}\left[\int_0^\infty e^{-rt}H_2(Y_t)I(Y_t \geq b_Y(X_t))dt\right]. \tag{5.9}$$

Explicit expressions for the premium components are in Lemma 7.1 in Appendix.

5.2. Extension B: Time to build

In this section, we take time-to-build, i.e., the time needed to build a plant once the investment decision has been made, into account. This delay is a source of losses as the firm cannot collect positive cash flows until the plant is built. To formalize this extension, we denote by $\Delta_g \geq 0$ and $\Delta_w \geq 0$ the corresponding time delays for the gas and wind plants, respectively. Let us first analyze the wind plant. The expected discounted value of profits is given by,

$$W(y) = \mathsf{E}_y\left[\int_{\Delta_w}^\infty e^{-rt}(s + Y_t - k_w)dt\right]$$

for $y > 0$ so that,

$$W(y) = \frac{e^{-\delta_Y\Delta_w}}{\delta_Y}y + \frac{e^{-r\Delta_w}(s - k_w)}{r}.$$

It is clear that when $\Delta_w = 0$ we are back to the main setting of the paper.

Now if we consider the gas-fired plant, the expression for the present value becomes more complicated due to possible switches in operational states. In particular, if investment is decided at time t, then the spread process may end up below b_1 at $t + \Delta_g$, in which case the plant is optimally in the idle state. The expected discounted value of profits is given by,

$$\mathsf{E}_x \left[e^{-r\Delta_g} \max(V_0(X_{\Delta_g}), V_1(X_{\Delta_g})) \right]$$

for $x \in I\!R$. If we expand this expectation using Ito's formula, there will be local time term and both the theoretical and numerical analyses become more involved. To avoid technical difficulties, we can use the following approximation: as entering into the gas-fired technology is only optimal for sufficiently large spread value, the likelihood that $X_{\Delta_g} < b_1$ is typically quite small and can be neglected. Thus, we can estimate the present value of profits as

$$\begin{aligned} \mathsf{E}_x \left[e^{-r\Delta_g} V_1(X_{\Delta_g}) \right] =& V_1(x) + \mathsf{E}_x \left[\int_0^{\Delta_g} e^{-ru}(-X_u + k_1) du \right] \\ =& B_1 e^{\widetilde{\alpha} x} + e^{-r\Delta_g} \frac{x + \mu_x/r - k_1}{r} \end{aligned}$$

for $x > b_1$, where we used Ito's formula and the expression for $V_1(x)$.

Given these adjustments, we see that it is straightforward to introduce time-to-build into the analysis, as we simply multiple affine terms by exponential factors. Thus, integral equations and the numerical algorithm to solve them are almost the same as for the main framework.

6. Conclusion

In this paper, we have examined the optimal investment in power production projects when two competing technologies, a gas-fired plant or a wind farm, are considered. We show that the immediate investment policy is characterized by a pair of boundaries satisfying a system of coupled integral equations of the Fredholm type and provide a new algorithm to compute its solution. The value of the investment project has an early investment premium representation consisting of two components, each tallying the local gains achieved when investment in a given technology is optimal. In this context, we show that it is always optimal to postpone investment when the values of the two plants are equal. This is true even if these values are arbitrarily large. In fact waiting is optimal as long as the underlying factors, the spark spread and the price of electricity, lie in a cone. Thus, waiting can be optimal even if the discrepancy between the individual project values becomes unboundedly large.

The possibility of using renewables to produce electricity has a significant impact on the value of power generation projects. The premium associated with renewables is an increasing function of the price of electricity and a decreasing function of the spark spread. This premium is large at typical values of the spark spread and the electricity price, and can easily double the value of a project. It can remain positive even when the price of natural gas decreases and the spark spread increases. This provides an economic rationale as to why renewables power generation remains competitive even in the face of sharp declines in the cost certain fossil fuels.

Our analysis provides additional perspective regarding the importance of renewables for modern societies. It is clear that renewables have a major role to play in alleviating the negative

consequences, such as global warming and other climate change phenomena, associated with reliance on fossil fuels. This study shows that renewables provide immediate financial benefits for power plant operators even if the economics of the problem would suggest that renewables are dominated by fossil fuels for power generation. The mere availability of power production based on renewables implies that it might be optimal to postpone investments and consider green power generation as a viable alternative to fossil fuel power generation.

7. Appendix

7.1. Appendix A: Proofs and numerical scheme

Proof of Theorem 4.1. (i) The existence of exercise boundaries is equivalent to the up-connectedness of $\mathcal{D}_w$ and the right-connectedness of $\mathcal{D}_g$. In other words, if $(x,y) \in \mathcal{D}_w \Longrightarrow (x,\lambda y) \in \mathcal{D}_w$ for $\lambda \geq 1$, and if $(x,y) \in \mathcal{D}_g \Longrightarrow (\lambda x, y) \in \mathcal{D}_g$ for $\lambda \geq 1$. Both implications follow by standard dominance arguments.

(ii) The functions $G_1(x)$ and $G_2(y)$ are both convex. The max-option payoff, as a composition of convex functions, is also convex. Convexity of the exercise subregions $\mathcal{D}_g$ and $\mathcal{D}_w$ follows. Hence both boundaries b_X and b_Y are convex (and thus continuous).

Monotonicity of the boundaries is equivalent to the the left-connectedness of $\mathcal{D}_w$ and down-connectedness of $\mathcal{D}_g$. The former fact can be shown as follows. Let us take $(x,y) \in \mathcal{D}_w$ and $\lambda \leq 1$, then $G(\lambda x, y) = G(x,y) = G_2(y)$ and $V(\lambda x, y) \leq V(x,y)$. Next, we have that $0 \leq V(\lambda x, y) - G(\lambda x, y) \leq V(x,y) - G(x,y) = 0$ and hence $V(\lambda x, y) = G(\lambda x, y)$, i.e., $(\lambda x, y) \in \mathcal{D}_w$, which proves left-connectedness of $\mathcal{D}_w$. Similar arguments show that $\mathcal{D}_g$ is right-connected.

(iii) This result is straightforward. When $y \to 0+$ or $x \to -\infty$, the selection option simply reduces to the single option on the wind plant or gas-fired plant, respectively,

$$\sup_{0\leq\tau\leq\infty} \mathsf{E}_x\left[e^{-r\tau}(V_g(X_\tau) - K_g)\right], \qquad \text{or} \qquad \sup_{0\leq\tau\leq\infty} \mathsf{E}_y\left[e^{-r\tau}(W(Y_\tau) - K_w)\right]$$

for $x \in I\!R$ and $y > 0$. Both problems are one-dimensional stopping problems, which can be solved using standard arguments. The optimal exercise strategies are given by constant thresholds b_X^g and b_Y^w. We then have that $b_X(0+) = b_X^g$ and $b_Y(-\infty) = b_Y^w$. Moreover, b_X^g and b_Y^w are lower bounds for b_X and b_Y, respectively. It is also clear that $b_X^g \geq \max(b_1, k_1 + rK_1)$ and $b_Y^w \geq \max(\delta_Y(K_w - \frac{s-k_w}{r}), rK_w - (s-k_w))$.

(iv) This fact follows from the observation that it is not optimal to enter at all along the curve $\widehat{y}$. Lower bounds were proven in (iii) above.

□

Proof of Theorem 4.2. Let us assume that the operator faces the finite maturity T selection option problem,

$$V(x,y;T) = \sup_{t\leq\tau\leq T} \mathsf{E}_{x,y}\left[e^{-r\tau}\max(V_1(X_\tau) - K_g, W(Y_\tau) - K_w)\right]$$

for $x \in I\!R$, $y > 0$ and $T > 0$. Then the same arguments as in Theorem xxx shows the existence of exercise surfaces $b_X^T(t,y)$ and $b_Y^T(t,x)$ for $t \in [0,T)$, $x \in I\!R$ and $y > 0$. Standard

arguments of American options pricing theory provides the early exercise premium representation, i.e., the decomposition of American-style derivative into the European counterpart and early exercise premium (see e.g. Detemple (2006)),

$$V(x,y;T) = V^e(x,y;T) + \pi(t,x;b_X^T, b_Y^T, T)$$

where V^e is the expected discounted payoff at T,

$$V(x,y;T) = \mathsf{E}_{x,y}\left[e^{-rT}\max(V_1(X_T) - K_g, W(Y_T) - K_w)\right]$$

and the early exercise premium depends on the exercise surfaces (b_X^T, b_Y^T) and given as follows,

$$\pi(x,y;b_X^T,b_Y^T,T) = \pi_1(x,y;b_X^T,T) + \pi_2(x,y;b_Y^T,T) \tag{7.1}$$

$$\pi_1(x,y;b_X^T,T) = -\mathsf{E}_{x,y}\left[\int_0^T e^{-rt}H_1(X_t)I(X_t \geq b_X^T(t,Y_t))dt\right] \tag{7.2}$$

$$\pi_2(x,y;b_Y^T,T) = -\mathsf{E}_{x,y}\left[\int_0^T e^{-rt}H_2(Y_t)I(Y_t \geq b_Y^T(t,X_t))dt\right] \tag{7.3}$$

for $x \in I\!R$, $y > 0$ and $T > 0$. We now let $T \to +\infty$, it is clear then that $V(x,y;T) \to V(x,y)$, $b_X^T(t,y) \to b_X(y)$ and $b_Y^T(t,x) \to b_Y(x)$ for any given t, x and y. The European part then vanishes as e^{-rT} dominates and $\pi(x,y;b_X^T,b_Y^T,T) \to \pi(x,y;b_X,b_Y)$ so that

$$V(x,y) = \pi(x,y;b_X,b_Y)$$

for $x \in I\!R$ and $y > 0$. If now insert $x = b_X(y)$ and $y = b_Y(x)$, respectively, we arrive at the system of two integral equations (4.2)-(4.3). □

The next lemma provides explicit formulas for the components of the EIP.

Lemma 7.1. *Under both ABM and OU models for the spark spread, the marginal distribution X_t has normal law with the mean $m(t,x)$ and standard deviation $std(t,x)$*

$$m(t,x) = x + \mu_X t \quad \& \quad std(t,x) = \sigma_X\sqrt{t} \quad \textit{(ABM model)}$$

$$m(t,x) = x\,e^{-\mu_X t} + \theta_X(1 - e^{-\mu_X t}) \quad \& \quad std(t,x) = \sqrt{\frac{\sigma_X^2}{2\mu_X}(1 - e^{-2\mu_X t})} \quad \textit{(OU model)}$$

for $t > 0$ and $x \in I\!R$. We then have the following expressions for π_1 and π_2

$$\begin{aligned}\pi_1(x,y;b_X) = &\int_0^\infty e^{-rt}(m(t,x) - k_1 - rK_1)\int_{-\infty}^\infty \varphi(z_1)\Phi\left(-\tfrac{h_1(z_1)-\rho z_1}{\sqrt{1-\rho^2}}\right)dz_1 dt \\ &+ \int_0^\infty e^{-rt}std(t,x)\int_{-\infty}^\infty \varphi(z_1)\left(\rho z_1\Phi\left(-\tfrac{h_1(z_1)-\rho z_1}{\sqrt{1-\rho^2}}\right) + \sqrt{1-\rho^2}\varphi\left(\tfrac{h_1(z_1)-\rho z_1}{\sqrt{1-\rho^2}}\right)\right)dz_1 dt\end{aligned} \tag{7.4}$$

$$\begin{aligned}\pi_2(x,y;b_Y) = &\int_0^\infty ye^{-\delta_Y t}\int_{-\infty}^\infty \varphi(z_2)\Phi\left(-\frac{h_{2,1}(z_2) - \rho z_2}{\sqrt{1-\rho^2}}\right)dz_2 dt \\ &+ \int_0^\infty e^{-rt}(s - rK_w)\int_{-\infty}^\infty \varphi(z_2)\Phi\left(-\frac{h_{2,2}(z_2) - \rho z_2}{\sqrt{1-\rho^2}}\right)dz_2 dt\end{aligned} \tag{7.5}$$

where $\varphi(\cdot)$ *and* $\Phi(\cdot)$ *are standard normal cdf and pdf, respectively, and the functions* $h_1, h_{2,1}$ *and* $h_{2,2}$ *are given by*

$$h_1(z) = \frac{1}{std(t,x)}\left(b_X\left(y\exp\left\{\left(\mu_Y - \tfrac{1}{2}\sigma_Y^2\right)t + \sigma_Y\sqrt{t}z\right\}\right) - m(t,x)\right) \tag{7.6}$$

$$h_{2,1}(z) = \frac{1}{\sigma_Y\sqrt{t}}\left(\log\left(\frac{b_Y\left(\widehat{m}(t,x) + std(t,x)z_2\right)}{y}\right) - \left(\mu_Y + \tfrac{1}{2}\sigma_Y^2\right)t\right) \tag{7.7}$$

$$h_{2,2}(z) = \frac{1}{\sigma_Y\sqrt{t}}\left(\log\left(\frac{b_Y\left(m(t,x) + std(t,x)z_2\right)}{y}\right) - \left(\mu_Y - \tfrac{1}{2}\sigma_Y^2\right)t\right) \tag{7.8}$$

for $z \in \mathbb{R}$ *and where* $\widehat{m}(t,x)$ *is defined as*

$$\widehat{m}(t,x) = x + (\mu_X + \rho\sigma_X)t \quad \textit{(ABM model)} \tag{7.9}$$

$$\widehat{m}(t,x) = x\,e^{-\mu_X t} + \frac{\mu_X\theta_X + \rho\sigma_Y}{\mu_X}\left(1 - e^{-\mu_X t}\right) \quad \textit{(OU model)} \tag{7.10}$$

for $t > 0$ *and* $x \in \mathbb{R}$ *.*

Proof of Lemma 7.1. We first note that we can rewrite $X_t = m(t,x) + std(t,x)\cdot B_1$ where $B_1 \sim N(0,1)$ under P. To prove the lemma, we calculate four different expectations.

1. Let us start with the following one,

$$\begin{aligned}\mathsf{E}_{x,y}\left[I(X_t \geq b_X(Y_t))\right] &= \mathsf{E}\left[I\left(m(t,x) + std(t,x)\cdot B_1 \geq b_X\left(ye^{\left(\mu_Y - \frac{1}{2}\sigma_Y^2\right)t + \sigma_Y Z_t}\right)\right)\right] \\ &= \mathsf{P}\left(B_1 \geq \frac{1}{std(t,x)}\left(b_X\left(ye^{\left(\mu_Y - \frac{1}{2}\sigma_Y^2\right)t + \sigma_Y Z_t}\right) - m(t,x)\right)\right) \\ &= \int_{-\infty}^{\infty}\int_{h_1(z_1)}^{\infty} f(z_1,z_2)dz_2dz_1\end{aligned} \tag{7.11}$$

where the function h_1 is defined in (7.6), and $f(z_1,z_2)$ is the joint density function of the normally distributed variables (B_1, Z_1) with zero mean, unit standard deviation and the correlation coefficient ρ. We can rewrite f as follows

$$f(z_1,z_2) = \varphi(z_1)\varphi_{2,1}(z_2|z_1) \tag{7.12}$$

where φ is the probability density function of standard normal variable Z_1 and $\varphi_{2,1}(\cdot|z_1)$ is the conditional density function of B_1 given that $Z_1 = z_1$. Let us calculate the latter function, for this we note that,

$$\begin{aligned}\mathsf{P}(B_1 \leq z_2|Z_1 = z_1) &= \mathsf{P}(\rho Z_1 + \sqrt{1-\rho^2}W \leq z_2|Z_1 = z_1) \\ &= \mathsf{P}\left(W \leq \frac{z_2 - \rho z_1}{\sqrt{1-\rho^2}}|Z_1 = z_1\right) \\ &= \mathsf{P}\left(W \leq \frac{z_2 - \rho z_1}{\sqrt{1-\rho^2}}\right) = \Phi\left(\frac{z_2 - \rho z_1}{\sqrt{1-\rho^2}}\right)\end{aligned} \tag{7.13}$$

where we used the decomposition $B_1 = \rho Z_1 + \sqrt{1-\rho^2}W$ with $W \sim N(0,1)$ independent of Z_1 and Φ is the cumulative distribution function of of standard normal law. By differentiating both sides of (7.13) w.r.t. z_2 , we obtain,

$$\varphi_{2,1}(z_2|z_1) = \frac{1}{\sqrt{1-\rho^2}}\varphi\left(\frac{z_2-\rho z_1}{\sqrt{1-\rho^2}}\right). \tag{7.14}$$

Now we return to the equation (7.11) above,

$$\begin{aligned}
\mathsf{E}_{x,y}\left[I(X_t \geq b_X(Y_t))\right] &= \int_{-\infty}^{\infty}\int_{h_1(z_1)}^{\infty} f(z_1,z_2)dz_2dz_1 \\
&= \int_{-\infty}^{\infty}\varphi(z_1)\int_{h_1(z_1)}^{\infty}\varphi_{2,1}(z_2|z_1)dz_2dz_1 \\
&= \int_{-\infty}^{\infty}\varphi(z_1)\int_{h_1(z_1)}^{\infty}\frac{1}{\sqrt{1-\rho^2}}\varphi\left(\frac{z_2-\rho z_1}{\sqrt{1-\rho^2}}\right)dz_2dz_1 \\
&= \int_{-\infty}^{\infty}\varphi(z_1)\int_{\frac{h_1(z_1)-\rho z_1}{\sqrt{1-\rho^2}}}^{\infty}\varphi\left(z_2\right)dz_2dz_1 \\
&= \int_{-\infty}^{\infty}\varphi(z_1)\Phi\left(-\frac{h_1(z_1)-\rho z_1}{\sqrt{1-\rho^2}}\right)dz_1
\end{aligned} \tag{7.15}$$

where in the second last equality we used the change-of-variables in the inner integral.

2. Now we simplify the second expectation,

$$\begin{aligned}
&\mathsf{E}_{x,y}\left[X_tI(X_t \geq b_X(Y_t))\right] \\
&=m(t,x)\mathsf{E}_{x,y}\left[I(X_t \geq b_X(Y_t))\right] \\
&\quad + std(t,x)\mathsf{E}_{x,y}\left[B_1\cdot I\left(x+\mu_X t+\sigma_X B_t \geq b_X\left(ye^{\left(\mu_Y-\frac{1}{2}\sigma_Y^2\right)t+\sigma_Y Z_t}\right)\right)\right] \\
&=m(t,x)\mathsf{E}_{x,y}\left[I(X_t \geq b_X(Y_t))\right] + std(t,x)\int_{-\infty}^{\infty}\int_{h_1(z_1)}^{\infty} z_2 f(z_1,z_2)dz_2dz_1 \\
&=m(t,x)\mathsf{E}_{x,y}\left[I(X_t \geq b_X(Y_t))\right] + std(t,x)\int_{-\infty}^{\infty}\varphi(z_1)\int_{h_1(z_1)}^{\infty} z_2\varphi_{2,1}(z_2|z_1)dz_2dz_1 \\
&=m(t,x)\mathsf{E}_{x,y}\left[I(X_t \geq b_X(Y_t))\right] + std(t,x)\int_{-\infty}^{\infty}\varphi(z_1)\int_{h_1(z_1)}^{\infty}\frac{z_2}{\sqrt{1-\rho^2}}\varphi\left(\frac{z_2-\rho z_1}{\sqrt{1-\rho^2}}\right)dz_2dz_1 \\
&=m(t,x)\mathsf{E}_{x,y}\left[I(X_t \geq b_X(Y_t))\right] + std(t,x)\int_{-\infty}^{\infty}\varphi(z_1)\int_{\frac{h_1(z_1)-\rho z_1}{\sqrt{1-\rho^2}}}^{\infty}(\rho z_1+z_2\sqrt{1-\rho^2})\varphi\left(z_2\right)dz_2dz_1 \\
&=m(t,x)\mathsf{E}_{x,y}\left[I(X_s \geq b_X(Y_t))\right] + \rho\cdot std(t,x)\int_{-\infty}^{\infty} z_1\varphi(z_1)\Phi\left(-\frac{h_1(z_1)-\rho z_1}{\sqrt{1-\rho^2}}\right)dz_1 \\
&\quad + \sqrt{1-\rho^2}\cdot std(t,x)\int_{-\infty}^{\infty}\varphi(z_1)\varphi\left(\frac{h_1(z_1)-\rho z_1}{\sqrt{1-\rho^2}}\right)dz_1
\end{aligned} \tag{7.16}$$

and the expectation $\mathsf{E}_{x,y}\left[I(X_t \geq b_X(Y_t))\right]$ is already computed above.

3. Here we turn to the third one,

$$
\begin{aligned}
(7.17)\qquad \mathsf{E}_{x,y}\left[I(Y_t \geq b_Y(X_t))\right] &= \mathsf{P}\left(ye^{\left(\mu_Y-\frac{1}{2}\sigma_Y^2\right)t+\sigma_Y Z_t} \geq b_Y\left(m(t,x)+std(t,x)B_1\right)\right) \\
&= \mathsf{P}\left(\left(\mu_Y-\tfrac{1}{2}\sigma_Y^2\right)t+\sigma_Y Z_t \geq \log\left(\frac{b_Y\left(m(t,x)+std(t,x)B_1\right)}{y}\right)\right) \\
&= \mathsf{P}\left(Z_1 \geq \frac{1}{\sigma_Y\sqrt{t}}\left(\log\left(\frac{b_Y\left(m(t,x)+std(t,x)B_1\right)}{y}\right)-\left(\mu_Y-\tfrac{1}{2}\sigma_Y^2\right)t\right)\right) \\
&= \int_{-\infty}^{\infty}\int_{h_{2,1}(z_2)}^{\infty} f(z_1,z_2)dz_1dz_2 \\
&= \int_{-\infty}^{\infty}\varphi(z_2)\Phi\left(-\frac{h_{2,1}(z_2)-\rho z_2}{\sqrt{1-\rho^2}}\right)dz_2
\end{aligned}
$$

where the function $h_{2,1}(z_2)$ is defined in (7.7).

4. Finally, we compute the remaining expectation,

$$
\begin{aligned}
(7.18)\qquad &\mathsf{E}_{x,y}\left[e^{-rt}Y_t I(Y_t \geq b_Y(X_t))\right] \\
&= y\,\widehat{\mathsf{E}}_{x,y}\left[e^{-\delta_Y t}I(Y_t \geq b_Y(X_t))\right] \\
&= ye^{-\delta_Y t}\widehat{\mathsf{P}}\left(\widehat{Z}_1 \geq \frac{1}{\sigma_Y\sqrt{t}}\left(\log\left(\frac{b_Y\left(\widehat{m}(t,x)+std(t,x)\widehat{B}_1\right)}{y}\right)-\left(\mu_Y+\tfrac{1}{2}\sigma_Y^2\right)t\right)\right) \\
&= ye^{-\delta_Y t}\int_{-\infty}^{\infty}\varphi(z_2)\Phi\left(-\frac{h_{2,2}(z_2)-\rho z_2}{\sqrt{1-\rho^2}}\right)dz_2
\end{aligned}
$$

where the function $h_{2,2}(z_2)$ is defined in (7.8) and in the first equality we changed the measure to $d\widehat{\mathsf{P}} = \exp\{\sigma_Y Z_t - \frac{\sigma_Y^2}{2}t\}d\mathsf{P}$ under which the process $\widehat{Z}_t = Z_t - \sigma_Y t$ is $\widehat{\mathsf{P}}$-SBM. We then represent $X_t = \widehat{m}(t,x) + std(t,x)\cdot\widehat{B}_1$ where $\widehat{B}_1$ is standard normal under $\widehat{\mathsf{P}}$ and $\widehat{m}(t,x)$ is given in (7.9)-(7.10). Both variables $\widehat{Z}_1$ and $\widehat{B}_1$ are standard normal with correlation ρ under $\widehat{\mathsf{P}}$, and we obtained the last equality by the adjusted calculations in step 3 above.

Now by combining the formulas in steps 1-4 above, we complete the proof. □

Proof of Proposition 4.3. Now we derive the asymptotic behavior of the boundaries at $+\infty$ Let us consider first the integral equation (4.2) and divide both sides by y, then letting $y \to +\infty$ and rearranging terms we get,

$$
(7.19)\qquad \lim_{y\to+\infty}\frac{b_X(y)}{y} = \frac{\lim_{y\to+\infty}\int_0^{\infty}e^{-\delta_Y t}\int_{-\infty}^{\infty}\varphi(z_2)\Phi\left(-\frac{h_{2,1}(z_2)-\rho z_2}{\sqrt{1-\rho^2}}\right)dz_2dt}{1/r - \lim_{y\to+\infty}\int_0^{\infty}e^{-rt}\int_{-\infty}^{\infty}\varphi(z_1)\Phi\left(-\frac{h_1(z_1)-\rho z_1}{\sqrt{1-\rho^2}}\right)dz_1dt}
$$

as all integrals are finite and most of the terms are dominated by y. As the right-hand side of (7.19) is finite, it implies that $b_X(y)$ is linear at infinity and this right-hand side gives the

slope b_X^∞ . To determine this slope we need to understand the limits of h_1 and $h_{2,1}$ as y goes to $+\infty$ and $x = b_X(y)$. From (7.6) and (7.7),

$$\lim_{y\to+\infty} h_1(z_1) = +\infty \cdot sign\left((\mu_Y - \tfrac{1}{2}\sigma_Y^2)t + \sigma_Y\sqrt{t}z_1\right) \tag{7.20}$$

$$\lim_{y\to+\infty} h_2(z_2) = \frac{1}{\sigma_Y\sqrt{t}}\left(\log\left(b_X^\infty b_Y^\infty\right) - \left(\mu_Y + \tfrac{1}{2}\sigma_Y^2\right)t\right) \tag{7.21}$$

and thus we rewrite (7.19) as,

$$b_X^\infty = \lim_{y\to+\infty}\frac{b_X(y)}{y} = \frac{\int_0^\infty e^{-\delta_Y t}\int_{-\infty}^\infty \varphi(z_1)\Phi\left(-\frac{\frac{1}{\sigma_Y\sqrt{t}}\left(\log(b_X^\infty b_Y^\infty) - \left(\mu_Y + \frac{1}{2}\sigma_Y^2\right)t\right) - \rho z_2}{\sqrt{1-\rho^2}}\right) dz_1\, dt}{1/r - \int_0^\infty e^{-rt}\int_{-\infty}^\infty \varphi(z_1) I\left(\left(\mu_Y - \frac{1}{2}\sigma_Y^2\right)t + \sigma_Y\sqrt{t}z_1 < 0\right) dz_1\, dt}. \tag{7.22}$$

Now we repeat the same procedure for (4.3) and obtain,

(7.23)

$$b_Y^\infty = \lim_{x\to+\infty}\frac{b_Y(x)}{x} = \frac{\int_0^\infty e^{-rt}\int_{-\infty}^\infty \varphi(z_1) I\left(b_X^\infty b_Y^\infty \exp\{\left(\mu_Y - \frac{1}{2}\sigma_Y^2\right)t + \sigma_Y\sqrt{t}z_1\} < 1\right) dz_1\, dt}{1/\delta_Y - \int_0^\infty e^{-\delta_Y t}\int_{-\infty}^\infty \varphi(z_2)\Phi\left(\frac{1}{\sqrt{1-\rho^2}}\left((\mu_Y/\sigma_Y + \sigma_Y/2)\sqrt{t} + \rho z_2\right)\right) dz_2\, dt}$$

and thus $b_Y(x)$ also has linear growth with linear slope b_Y^∞ . Now multiplying equations (7.22) and (7.23), we derive the equation (4.7) for $b^\infty = b_X^\infty b_Y^\infty$. Having obtained b^∞ as the unique root, we determine b_X^∞ and b_Y^∞ from (7.22) and (7.23).

Finally, lower bounds for b_X and b_Y follow from the fact that exercise boundaries are convex. □

Numerical scheme. Here we describe the numerical scheme we exploited to produce the numerical results in Section 4.5. The main goal is to solve numerically the system of integral equations (4.2)-(4.3).

As the both boundaries b_X and b_Y are defined on unbounded state spaces, we first have to truncate these spaces. Let us define bounded intervals $[0, Y_{max}]$ and $[X_{min}, X_{max}]$ for some large enough $Y_{max} > 0$, $X_{min} < 0$ and $X_{max} > 0$. We will compute b_X on $[0, Y_{max}]$ and b_Y on $[X_{min}, X_{max}]$. Next, we discretize both intervals, i.e., we choose integers $N_Y > 0$ and $N_X > 0$ to define the grids on intervals $[0, Y_{max}]$ and $[X_{min}, X_{max}]$ with step size $h_Y = Y_{max}/N_Y$ and $h_X = (X_{max} - X_{min})/N_X$.

We will compute sequences of boundaries $b_X^n(y_i)$ and $b_Y^n(x_j)$ for each $i = 1, ..., N_Y$ and $j = 1, ..., N_X$ where $y_i = ih_Y$ and $x_j = jh_X + X_{min}$. We define initial boundaries (b_X^0, b_Y^0)

$$b_X^0(y) = \begin{cases} b_X^g, & y < b_X^g/b_X^\infty \\ b_X^\infty \cdot y, & y \geq b_X^g/b_X^\infty \end{cases} \quad \text{and} \quad b_Y^0(x) = \begin{cases} b_Y^w, & x < b_Y^w/b_Y^\infty \\ b_Y^\infty \cdot x, & x \geq b_Y^w/b_Y^\infty. \end{cases}$$

This choice provides the best known lower bounds for both boundaries and should help to decrease the number of iterations required.

Now let us assume that we already computed the pair of boundaries $(b_X^{n-1}(y_i), b_Y^{n-1}(x_j))$ for each i and j . We then interpolate them linearly on the intervals (y_{j-1}, y_j) and (x_{i-1}, x_i) ,

respectively. We also extrapolate linearly beyond Y_{max} and outside of $[X_{min}, X_{max}]$. Now the main goal is to perform iteration and calculate $(b_X^n(y_i), b_Y^n(x_j))$ for each i and j. For this we solve both equations (4.8)-(4.9) separately using, e.g., the Newton-Raphson method. In fact, as G_2 is affine in y, we have an explicit expression for $b_Y^n(x_j)$. The same is not true for G_1, because of its nonlinear structure, so that we have to solve that algebraic equation. The right-hand sides of (4.8)-(4.9) are known as they depend only on $(b_X^{n-1}(y_i), b_Y^{n-1}(x_j))$ and those are already computed by the assumption of induction. The expressions for π_1 and π_2 are given explicitly in Lemma 7.1. We note that computation requires two-dimensional integration with respect to dt and dz on unbounded space. For this, we use the truncations $[0, T_{max}]$ and $[-Z_{max}, Z_{max}]$ for large enough $T_{max} > 0$ and $Z_{max} > 0$, and we discretize these with grid sizes $h_T = T_{max}/N_T$ and $h_Z = Z_{max}/N_Z$.

Having all the ingredients to extract the pair of boundaries $(b_X^n(\cdot), b_Y^n(\cdot))$ from (4.8)-(4.9), we then iterate for $n = 1, 2, ...$ until the variation $\max\left(\left\|b_X^n(\cdot) - b_X^{n-1}(\cdot)\right\|, \left\|b_Y^n(\cdot) - b_Y^{n-1}(\cdot)\right\|\right)$ falls below some tolerance threshold $\varepsilon > 0$. Standard arguments show that by letting all Y_{max}, N_Y, X_{min}, X_{max}, N_X, T_{max}, N_T, Z_{max}, N_Z, n go to $+\infty$ and ε to 0, we have that $\|b_X^n(\cdot) - b_X(\cdot)\| \to 0$.

7.2. Appendix B: Alternative model

In this section, we present an alternative model where we directly specify the dynamics of both gas and electricity prices. To achieve tractability for the gas plant problem, we however do not allow for operational flexility.

1. *Model.* We propose the model where both electricity (X) and gas (Y) prices are represented by geometric Brownian motion processes,

$$\begin{aligned} dX_t &= \mu_X X_t dt + \sigma_X X_t dW_t, \quad X_0 = x, \\ dY_t &= \mu_Y Y_t dt + \sigma_Y Y_t dZ_t, \quad Y_0 = y, \end{aligned}$$

where (W, Z) are standard Brownian motions positively correlated with parameter $|\rho| \leq 1$, and the parameters μ_A and $\sigma_A > 0$ represent the expected return and the return volatility, respectively, for $A = \{X, Y\}$. We can rewrite $\mu_A = r - \delta_A$, where $\delta_A > 0$ is an implicit yield for gas or electricity.

The production model assumes that both the gas and wind plants can operate indefinitely and that they always operate at full capacity. Their values are the present values of profits,

$$\begin{aligned} V(x, y) &= \mathsf{E}_{x,y}\left[\int_0^\infty e^{-rt}(X_t - Y_t - k)dt\right] \\ W(x) &= \mathsf{E}_x\left[\int_0^\infty e^{-rt}(s + X_t - k_w)dt\right] \end{aligned}$$

for $x, y > 0$. Straightforward computations give,

$$\begin{aligned} V_g(x, y) &= \frac{1}{\delta_X}x - \frac{1}{\delta_Y}y - \frac{k}{r} \\ W(x) &= \frac{1}{\delta_X}x + \frac{s - k_w}{r} \end{aligned}$$

for $x, y > 0$. Hence, in this case, both value functions are affine in state variables.

2. *Selection option.* Now we turn to the option to choose between the two types of plants with payoff,

$$G(x,y) = \max\{V_g(x,y) - K_g, W(x) - K_w\}$$

where $K_g > 0$ and $K_w > 0$, as before, represent the sunk costs for a gas-fired system and a wind plant, respectively.

The operator chooses the timing τ of the investment. The value of the license to build a power plant, either gas-fired or wind-based, is therefore given by,

$$V(x,y) = \sup_{0 \le \tau \le \infty} \mathsf{E}_{x,y}\left[e^{-r\tau} G(X_\tau, Y_\tau)\right]$$

for $x, y > 0$.

It is clear that the gas plant is preferred when the gas price is relatively cheap and that the wind plant is best for high gas prices. We now define an important threshold for the gas price,

$$\widehat{y} = \delta_Y \left(\frac{k_w - s - k}{r} + K_w - K_g \right)$$

so that,

$$G(x,y) = G_1(x,y) := \frac{1}{\delta_X} x - \frac{1}{\delta_Y} y - \frac{k}{r} - K_g$$

for $y \le \widehat{y}$ and $x > 0$, and

$$G(x,y) = G_2(x) := \frac{1}{\delta_X} x + \frac{s - k_w}{r} - K_w$$

for $y > \widehat{y}$ and $x > 0$.

As in our main model, it is optimal to wait along the indifference curve, which in this case is the vertical line $\{(y,x) : y = \widehat{y}\}$. Using standard arguments, we can show that there exist two boundaries $b_1(y)$ and $b_2(y)$ on $(0, \widehat{y})$ and $(\widehat{y}, \infty)$, respectively, so that it is optimal to enter into the gas plant when $x \ge b_1(y)$ for $y < \widehat{y}$ and into the wind plant when $x \ge b_2(y)$ for $y > \widehat{y}$. It can be also shown that b_1 is increasing with limit $b_1(\widehat{y}-) = +\infty$ and b_2 is decreasing with $b_2(\widehat{y}+) = +\infty$. We also have that $b_1(0+) = ...$ and $b_2(+\infty) = ...$, as in both cases the selection problem reduces to an standard call option problem for gas and wind plant, respectively.

3. *Integral equations.* By using similar arguments as in Theorem 4.2, we can prove that the pair of investment boundaries (b_1, b_2) solves the pair of coupled integral equations,

$$G_1(b_1(y), y) = \pi(b_1(y), y; b_1, b_2) \tag{7.24}$$

$$G_2(b_2(y)) = \pi(b_2(y), y; b_1, b_2) \tag{7.25}$$

on $(0, \widehat{y})$ and $(\widehat{y}, \infty)$, respectively, where $\pi(x, y; b_1, b_2)$ represents the early investment premium (EIP) defined as,

$$\pi(x, y; b_1, b_2) = \pi_1(x, y; b_1) + \pi_2(x, y; b_2) \tag{7.26}$$

$$\pi_1(x,y;b_1) = \mathsf{E}_{x,y}\left[\int_0^\infty e^{-rt}(X_t - Y_t - k - rK_1)I(X_t \geq b_1(Y_t))dt\right] \tag{7.27}$$

$$\pi_2(x,y;b_2) = \mathsf{E}_{x,y}\left[\int_0^\infty e^{-rt}(X_t + s - k_w - rK_2)I(X_t \geq b_2(Y_t))dt\right] \tag{7.28}$$

for $x, y > 0$.

4. *Numerical scheme.* As for the main model, we make use of the following iterative procedure. Let us choose some initial curves $(b_1^0(y), b_2^0(y))$ for $(0, \widehat{y})$ and $(\widehat{y}, \infty)$, respectively, and then, recursively, define $b_1^n(y)$ and $b_2^n(y)$ as follows,

$$b_1^n(y) = \delta_X\left(\pi(b_1^{n-1}(y), y; b_1^{n-1}, b_2^{n-1}) + \frac{1}{\delta_Y}y + \frac{k}{r} + K_g\right) \tag{7.29}$$

$$b_2^n(y) = \delta_X\left(\pi(b_2^{n-1}(y), y; b_1^{n-1}, b_2^{n-1}) - \frac{s - k_w}{r} + K_w\right) \tag{7.30}$$

for $y \in (0, \widehat{y})$ and $y \in (\widehat{y}, \infty)$, respectively, and $n \geq 1$. We can define initial values as $b_1^0(y) \equiv b_1(0+)$ on $(0, \widehat{y})$ and $b_2^0(y) \equiv b_2(+\infty)$ on $(\widehat{y}, \infty)$. We then iterate for $n = 1, 2, ...$ until the variation $\left(b_1^n(y) - b_1^{n-1}(y), b_2^n(y) - b_2^{n-1}(y)\right)$ falls below a predetermined tolerance threshold.

References

[1] Boomsma, T.K., Meade, N. and S-E. Fleten (2012). Renewable Energy Investments under Different Support Schemes: A Real Options Approach. *European Journal of Operational Research* 220(1), 225–237.

[2] Brennan, M. and E.S. Schwartz (1985). Evaluating Natural Resource Investments. *Journal of Business* 58(2), 135-157.

[3] Broadie, M. and J. Detemple (1997). The Valuation of American Options on Multiple Assets. *Mathematical Finance* 7(3), 241-285.

[4] Carr, P., Jarrow, R. and R. Myneni (1992). Alternative Characterizations of American Put Options. *Mathematical Finance* 2(2), 87–106.

[5] Deng, S., Johnson, B. and A. Sogomonian (1999). Spark Spread Options and the Valuation of Electricity Generation Assets, *Proceedings of the 32nd Hawai International Conference on System Sciences*, 1-7.

[6] Detemple, J. (2006). *American-Style Derivatives.* Chapman & Hall/CRC.

[7] Dixit, A.K. and R.S. Pindyck (1994). *Investment under Uncertainty*, Princeton University Press: Princeton, NJ.

[8] Fleten, S-E. and E. Näsäkkälä (2004). Gas Fired Power Plants: Investment Timing, Operating Flexibility and Abandonment. Working Paper, University of München.

[9] Fleten, S-E., Maribu, K.M. and I. Wangensteen (2007). Optimal Investment Strategies in Decentralized Renewable Power Generation under Uncertainty. *Energy* 32(5), 803–815.

[10] Geman, H. and A. Roncoroni (2006). Understanding the Fine Structure of Electricity Prices. *Journal of Business* 79(3), 1225-1261.

[11] Kim, I.J. (1990). The Analytic Valuation of American Options. *Review of Financial Studies* 3(4), 547–572.

[12] Lucia, J.J. and E.S. Schwartz (2002). Electricity Prices and Power Derivatives: Evidence from the Nordic Power Exchange. *Review of Derivatives Research.* 5(1), 5–50.

[13] Maribu, K.M., Galli, A. and M. Armstrong (2007). Valuation of Spark-spread Options with Mean Reversion and Stochastic Volatility. *International Journal of Electronic Business Management* 5(3), 173-181.

[14] McDonald, R. and D. Siegel (1985). Investment and the Valuation of Firms when there is an Option to Shut Down. *International Economics Review* 26(2), 331-349.

[15] McDonald, R. and D. Siegel (1986). The Value of Waiting to Invest. *Quarterly Journal of Economics* 101(4), 707-727.

[16] Peskir, G. (2005). A Change-of-Variable Formula with Local Time on Curves. *Journal of Theoretical Probability* 18(3), 499-535.

[17] REN21 (2016). Renewables 2016 Global Status Report.